Wang, Z. Z., Bertola, N. J., Goh, S. H., & Smith, I. F. C. (2021). Systematic selection of field response measurements for excavation back analysis. *Advanced Engineering Informatics*, *48*, 101296. https://doi.org/https://doi.org/10.1016/j.aei.2021.101296

Systematic Selection of Field Response Measurements for Excavation Back Analysis

Ze Zhou WANG[a, b, *]; Numa Joy BERTOLA [b, c]; Siang Huat GOH[a, b]; Ian F.C. SMITH[b, c]

a. Department of Civil & Environmental Engineering, National University of Singapore, Block E1A, #07-03, No.1 Engineering Drive 2, Singapore 117576. Email: e0054291@u.nus.edu (WANG, Ze Zhou); gohsianghuat@nus.edu.sg (GOH, Siang Huat);

b. Future Cities Laboratory, Singapore-ETH Centre, 1 CREATE Way, CREATE Tower, #06-01, Singapore 138602, Singapore.

c. Applied Computing and Mechanics Laboratory (IMAC), School of Architecture, Civil and Environmental Engineering (ENAC), Swiss Federal Institute of Technology (EPFL), Lausanne, Switzerland. Email: ian.smith@epfl.ch (Ian F.C. SMITH); numa.bertola@epfl.ch (Numa Joy BERTOLA)

Corresponding author:

WANG, Ze Zhou

Email: e0054291@u.nus.edu

Postal address: Future Cities Laboratory, Singapore-ETH Centre, 1 Create Way, CREATE Tower, #06-01, Singapore 138602

Wang, Z. Z., Bertola, N. J., Goh, S. H., & Smith, I. F. C. (2021). Systematic selection of field response measurements for excavation back analysis. *Advanced Engineering Informatics*, *48*, 101296. https://doi.org/https://doi.org/10.1016/j.aei.2021.101296

Systematic Selection of Field Response Measurements for Excavation Back Analysis

Ze Zhou WANG; Numa Joy BERTOLA; Siang Huat GOH; Ian F.C. SMITH;

Abstract:

In a geotechnical excavation, back analyses are routinely performed using the measured field responses to derive the material parameter values for the different soil layers present at the site. For the purpose of back analyses, the engineers will usually make use of a portion of the large volumes of field data collected, in order to keep the computational effort to a manageable level. However, excavation back analyses using different selected sets of field response measurements may not yield the same knowledge of material parameter values. Therefore, measurements need to be carefully selected to obtain the best estimates of material parameter values. Currently, the selection of measurements is largely based on engineering heuristics; no method has been proposed to systematically quantify the expected knowledge of the parameter values that field response measurements could provide. In this paper, a hierarchical algorithm based on a joint-entropy objective function is proposed to systematically evaluate the knowledge gained from wall deflections measured by eight inclinometers at an excavation site. The algorithm ranks the inclinometers based on the expected knowledge yield of the parameter values. Back analysis using actual field response measurements is then carried out to corroborate the ranking. The rankings obtained from the back analysis results and the predictions of the hierarchical algorithm are very similar, which suggests that the latter method can aid in the judicious selection of field response measurements in order to obtain useful knowledge of material parameter values. Since the application of the hierarchical algorithm does not entail the use of actual measurements, such predictions can be made at the early stages of a project, even before the commencement of site activities.

Keywords: Information entropy; Joint entropy; Hierarchical algorithm; Back analysis; Finite-element analysis; Geotechnical excavation;

1. Introduction

The combination of various geologic, chemical, physical and environmental processes has made soil a material that has high variability in mechanical properties. Such variability creates challenges to the design and analysis of geotechnical structures [31, 39, 42]. While knowledge pertaining to soil properties can be obtained from laboratory tests on soil samples, other strategies that involve machine learning and utilization of big data have also been proposed [20, 43, 47]. One of the alternative strategies for gaining knowledge of soil properties is through measurement of behaviour and back analysis. A back analysis, which is synonymous with system identification or model updating, is performed using measured field responses to obtain knowledge pertaining to material parameter values [8, 14, 15, 16, 41, 45, 51, 52, 57, 58], from which engineers can make informed decisions and achieve better designs.

In an excavation project, the measurements typically consist of inclinometer readings that capture the retaining wall deflections, as well as survey data from the movement of ground settlement markers. Due to variations in natural ground conditions that are encountered at almost all sites, the inclinometers and ground settlement markers are usually installed at multiple locations within the excavation site. Depending on the scale of the project, the measurement data collected can be quite voluminous. For the purpose of back analyses, the engineers will usually make use of data from only a selected number of instruments, in order to keep the computational effort to a manageable level. The extra data that are collected but not used serve as redundancies or back-up information in the event of sensor break-down or malfunction, which are quite common occurrences. In this regard, a trade-off may be necessary when field response measurements need to be selected for a back analysis. This involves the consideration of two issues.

First, the data measured at several locations of an engineering structure do not necessarily provide the same knowledge pertaining to the material parameter values [32] and therefore, field response measurements of multiple sensors are usually involved in a back analysis. However, mutual information about the material parameter values can also exist among measurement data from various sensors. Mutual information occurs when the knowledge about the material parameter values obtained using the data of one sensor is similar to that obtained using the data of another sensor. As a result, one sensor is considered to be redundant for a back analysis because it provides limited improved knowledge of material parameter values. This has led to the second issue, which is that the inclusion of more measurement data does not necessarily lead to proportionate gains in knowledge of material parameter values [4, 16]. In the worst case, it can lead to less effective identification of material parameter values [12]. Hence, the proper selection and adoption of field response measurements collected at appropriate inclinometer locations is important to obtain the maximum useful information of material parameter values from back analysis.

Previous work on excavation back analysis either utilised as much measurement data as was available [16, 18, 49] or considered only selected measurement data based on engineering judgement [14, 41, 45, 56]. In many cases, wall deflections measured at the middle section of an excavation are usually chosen because these magnitudes are typically the largest and are best approximated by plane strain condition. If wall deflections measured at several locations are used simultaneously, most studies do not use data from more than one inclinometer located on the same side of the excavation [15, 41]. While this may be intended to reduce redundant information provided by the inclinometers, the selection of which data set to use does not appear to be based on any quantitative approach. To date, no systematic method has been proposed to provide guidance on the optimal selection of excavation measurement data from multiple inclinometer readings for excavation back analysis.

In the present study, a hierarchical algorithm based on a joint-entropy objective function is adopted to systematically evaluate the information provided by field response measurement data. It is worth mentioning that the knowledge of material parameter values and excavation behaviour is defined loosely in this introductory section. In the later part of this paper, specific aspects of the back analysis results will be selected to represent the knowledge of material parameter values and excavation behaviour.

Papadimitriou et al. [32] originally introduced information entropy from information theory as a sensor-placement objective function in the field of structural identification. Information entropy can be either minimized in posterior model-parameter distributions [33] or maximized in model-population prediction [40]. Most work uses greedy algorithms to reduce the computation time of the optimization task, such as [21] among many others.

As suboptimal solutions may be obtained if the mutual information is not properly taken into account in the optimization phase [54], Papadopoulou et al. [35] introduced a hierarchical algorithm based on a joint-entropy objective function that explicitly evaluates the mutual information between sensors. While it was originally implemented for the study of wind predictions around buildings, this algorithm has been successfully modified and implemented to civil engineering applications such as water-pipe leak detection [28] and bridge engineering [4]. Other than the hierarchical algorithm, some studies investigated optimal measurement systems using the value of the information collected through utility theory [36], value of information [26] and multi-criteria decision analysis framework [6].

The selection of potential field response measurements using the hierarchical algorithm does not entail the use of any actual measurements from the field excavation. Therefore, such an exercise can be carried out at an early stage of the project to help identify useful measurements for back analysis. An excavation case history in Singapore is used to illustrate the effectiveness of the methodology. Eight inclinometers were installed for the excavation, each measuring wall deflections at 1 m interval from ground level to the toe of the wall. The hierarchical algorithm is first used to rank the inclinometers based on the expected information represented by the value of joint-entropy. For comparison with the hierarchical algorithm's ranking, back analyses of the excavation are then carried out to examine how the use of selected wall deflection measurements from various combinations of single and multiple inclinometers affect the performance of the parameter identification process. Both the back analysis and the hierarchical algorithm produce similar inclinometer rankings, which suggests that the latter method can serve as a tool to select useful field response measurements that lead to the best information prior to a back analysis.

The hierarchical algorithm is formulated based on a recent population-based data-interpretation approach known as error-domain model falsification (EDMF) [12]. Due to the large number of simulations required, the response surface method is adopted to facilitate the computations of both the hierarchical algorithm and the back analyses. The response surfaces are used to replace the 2D finite element models of the excavation. However, as will be shown later in Figure 4, some inclinometers are located near to excavation corners and therefore, the 2D model may not be adequate. The approach proposed by Wang et al. [51] to quantify three-dimensional excavation effects is then adopted to facilitate the analyses of these inclinometers. More details regarding the two techniques will be provided in the later part of this paper.

2. Methodologies

2.1. Error-domain model falsification

This method was developed based on the assertion of Sir Karl Popper in *The Logic of Scientific Discovery* [34] that models cannot be fully validated by data and that they can only be falsified. In the context of EDMF, a model, e.g. a FEM model, is first constructed to represent the studied engineering structure. Then, the analysis proceeds to the generation of an initial population of material parameter value sets. This initial population of material parameter value sets, referred as "instances/model instances" in the subsequent parts of this paper, are inputs of the FEM model for predicting the responses of the engineering structure. Such a model-instance set defines the model class of the studied engineering structure [46]. The falsification process is then carried out to eliminate parameter value sets that do not yield predictions compatible with field response measurements, based on some pre-defined acceptance criteria. The remaining non-falsified parameter value sets, which are termed candidates, are considered as viable inputs for use with the numerical model to assess the behaviour of the actual system. In this regard, EDMF often yields a solution that comprises a population of candidates. The more detailed mathematical formulation is provided below.

A plausible physics-based model defined by n_θ parameter values and a model class G_k can be identified using field response measurements. In the context of an excavation problem, a retaining wall deflection profile taken by an inclinometer at n_y number of measurement locations is often adopted in the identification process. Let R_i and $\hat{y}_i$ denote the real response and the measured response respectively at location $i \in \{1, \ldots, n_y\}$. Predictions $g_{i,k}(\Theta'_k)$ of the model class at location i can be obtained using values for Θ'_k, which correspond to the true parameter values. Modelling uncertainties arising from model simplifications/omissions and measurement uncertainties are expressed as $U_{i,gk}$ and $U_{i,\hat{y}}$ respectively at location i. The mathematical relationship between these quantities is given in Eq. (1):

$$g_{i,k}(\Theta'_k) + U_{i,g_k} = R_i = \hat{y}_i + U_{i,\hat{y}} \quad \forall_i \in \{1,\ldots,n_y\} \tag{1}$$

Upon rearrangement, Eq. (2) is obtained:

$$g_{i,k}(\Theta'_k) - \hat{y}_i = U_{i,ck} \tag{2}$$

where $U_{i,ck}$ is a random variable representing the difference between the measurement uncertainty $U_{i,\hat{y}}$ and the modelling uncertainty $U_{i,gk}$ at location i.

The left term of Eq. (2) is typically called the residual r_i, which represents the difference between the model prediction and the measurement at location i. The implementation of EDMF starts with the generation of n_Ω model instances $\Omega_k = \{\Theta_{k,m}, \mathrm{m} = 1,\ldots, n_\Omega\}$. Threshold bounds are then defined by computing the narrowest interval $\{u_{ik,low}, u_{ik,high}\}$ that represents a probability equal to $\emptyset_d^{1/n_v}$ for the combined PDFs $f_{Ui,ck}(u_{i,ck})$ at each measurement location i. This computation is performed using the following equation:

$$\emptyset_d^{1/n_v} = \int_{u_{ik,low}}^{u_{ik,high}} f_{u_{i,ck}}\left(u_{i,ck}\right) du_{i,ck} \quad \forall_i \in \{1,\ldots,n_v\} \tag{3}$$

The combined PDFs $f_{Ui,ck}(u_{i,ck})$ at each measurement location i is obtained using numerical sampling [12]. Error samples are drawn from several uncertainty probability density functions and then added together. A value of 0.95 for the confidence level $\emptyset_d \in [0,1]$ is commonly employed. The confidence level $\emptyset_d$ is adjusted using the Šidák correction [44] to take into account the fact that n_v measurements are used simultaneously. For example, assuming that there are two measurement locations, each of which is associated with an uncertainty that is normally distributed with a mean of 0 and a standard deviation of 1, the adjusted confidence level at each measurement location is $0.95^{1/2} = 0.9747$. Therefore, the $u_{ik,low}$ and $u_{ik,high}$ at each measurement location bound the PDF of the uncertainty distribution with an area of 0.9747. Uniform probability distributions are then assigned to the lower and upper bounds calculated to create a hyper-rectangular acceptance region. Under this scheme, the value of the correlation between measurement locations is no longer needed, which is particularly important because

Wang, Z. Z., Bertola, N. J., Goh, S. H., & Smith, I. F. C. (2021). Systematic selection of field response measurements for excavation back analysis. *Advanced Engineering Informatics*, *48*, 101296. https://doi.org/https://doi.org/10.1016/j.aei.2021.101296

it is often difficult to determine the correlation values between measurement locations. Falsification is then performed according to the following equation:

$$\Omega_k'' = \{\Theta_k \in \Omega_k \mid \forall_i \in \{1,\ldots,n_v\}\ u_{ik,low} \leq g_{i,k}(\Theta_k) - \hat{y}_i \leq u_{ik,high}\} \quad (4)$$

An instance Θ^*_k of a model class G_k is a candidate if for each measurement location $i \in \{1, \ldots, n_v\}$, the residual r_i value falls inside the threshold bounds derived from Eq. (3). The candidate set (CMS), Ω_k'', is then made up of all model instances that have not been falsified. A uniform probability distribution is assigned to all model instances that belong to the CMS because it is often difficult to justify a more sophisticated distribution in practical situations. Details of EDMF implementation on a multi-stage excavation problem can be found in [50, 51, 52].

2.2. Hierarchical algorithm

2.2.1. Original implementation [35]

Papadopoulou et al. [35] introduced a hierarchical algorithm based on a joint-entropy objective function that explicitly evaluates the mutual information between sensors. Information entropy from information theory is the "amount of information" contained in a variable or an event. In the current analysis, the event is the back analysis while the information is the knowledge of the material parameter values and the excavation behaviour. Section 5 will provide a detailed definition of "knowledge" in the current study.

The hierarchical algorithm involves several steps. A FEM model is first constructed, which is used to generate the predictions at each sensor location corresponding to an input population of material parameter combinations. A total of 1000 material parameter combinations is used in the present study, these being generated using the Latin Hypercube sampling technique. It is also necessary to estimate the modelling uncertainties and instrumentation errors associated with this problem. Using the FE predicted datasets and the quantified uncertainties, the expected gain in knowledge about the material parameter values, represented as information entropy, is evaluated.

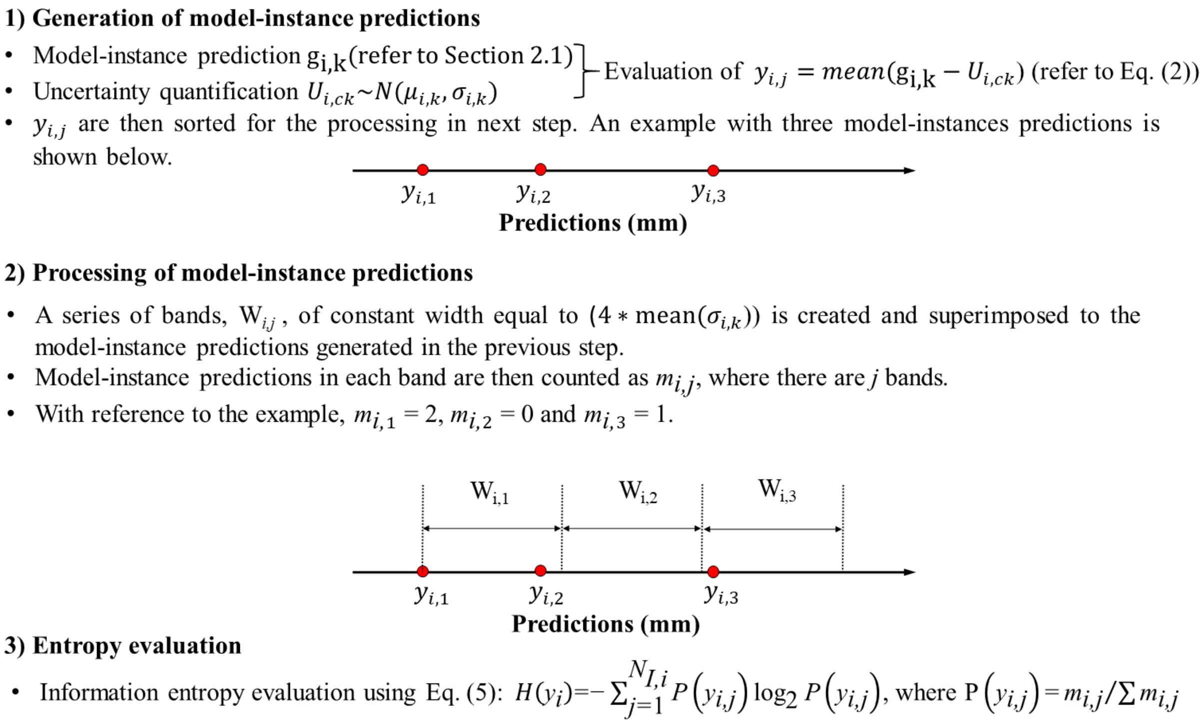

Figure 1 An illustration on the procedures of the hierarchical algorithm.

With reference to Figure 1, at each sensor location *i*, prediction datasets generated from the FE analyses are first generated. This is shown in step 1) in Figure 1. Then, a series of bands are generated based on the combined uncertainties in Eq. (2). The width of each band is constant and is proportional to the difference between the lower and upper threshold bounds computed by Eq. (3). This is shown in step 2) in Figure 1. In the next step, for each sensor location *i,* the probability that the model-instance prediction falls inside the j^{th} band, denoted as $P(y_{i,j})$, equals to $m_{i,j}/\sum m_{i,j}$, where $m_{i,j}$ is the count of model instances inside the j^{th} band. The information entropy $H(y_i)$ can then be evaluated using Eq. (5).

Wang, Z. Z., Bertola, N. J., Goh, S. H., & Smith, I. F. C. (2021). Systematic selection of field response measurements for excavation back analysis. *Advanced Engineering Informatics*, *48*, 101296. https://doi.org/https://doi.org/10.1016/j.aei.2021.101296

$$H\left(y_i\right) = -\sum_{j=1}^{N_{I,i}} P\left(y_{i,j}\right) \log_2 P\left(y_{i,j}\right) \tag{5}$$

When more than one sensor is present in a measurement system, there is likely to be some redundancy of information gain between sensors, also known as mutual information. To explicitly account for mutual information, Papadopoulou et al. [35] proposed joint entropy as a new objective function to quantify the redundancy of information gain between sensors. The joint entropy $H(y_{i,i+1})$ assesses the information entropy between sets of predictions, such as between two sensors, which allows the consideration of redundancy of information gain between sensors. For a set of two sensors, the joint entropy is defined using Eq. (6), where $P(y_{i,j}, y_{i+1,k})$ is the joint probability that a model instance falls inside the j^{th} band at the sensor location i, and the k^{th} band at sensor location i+1, $k \in \{1, \dots, N_{I,i+1}\}$, $N_{I,i+1}$ is the maximum number of prediction band at the sensor location i+1 and $i+1 \in \{1, \dots, n_s\}$ with the total number of sensor locations n_s.

$$H(y_{i,i+1}) = -\sum_{k=1}^{N_{I,i+1}} \sum_{j=1}^{N_{I,i}} P(y_{i,j}, y_{i+1,k}) \log_2 P(y_{i,j}, y_{i+1,k}) \tag{6}$$

The joint entropy is less than or equal to the sum of the individual information entropies of multiple sets of predictions. Eq. (7) shows the joint entropy of two sensors, where $I(y_{i,i+1})$ is the mutual information between sensor i and i+1.

$$H(y_{i,i+1}) = H(y_i) + H(y_{i+1}) - I(y_{i,i+1}) \tag{7}$$

The hierarchical algorithm is a greedy search sequential algorithm [35] that selects sensors iteratively, in which the sensors previously selected are not re-evaluated during subsequent selections. At each iteration, the hierarchical algorithm re-evaluates only the joint-entropy objective function of the remaining sensors and chooses the one that maximises the joint entropy. The algorithm stops when all sensors are selected, providing a ranking of the sensors and an evaluation of the incremental information gain associated with each sensor.

2.2.2. Adaptation to excavation back analysis

In the current work, lateral wall deflections measured by inclinometers are examined. An inclinometer, installed at a designated location, typically measures the lateral deflections at every 1 m interval from the toe to the top of the retaining wall. As such, an inclinometer produces a set of readings at multiple depths. As excavations usually involve multiple stages, such a set of readings is recorded for every excavation stage. For the remainder of this paper, "inclinometer location" refers to the location at which the inclinometer is placed while "measurement" refers to the survey point reading at a depth and an excavation stage within each inclinometer-measured deflection profile. For example, a 10 m long inclinometer produces 40 measurements over 4 excavation stages.

As a simplification, the upper and lower threshold bounds are calculated based on the average values of the combined uncertainties and instrumentation errors. Figure 1 shows a simple example to illustrate this simplification. Three model instances with their corresponding values of $y_{i,1}$, $y_{i,2}$, and $y_{i,3}$ at location i are shown. Three bands, the width of which, denoted as $W_{i,j}$, is calculated using Eq. (3) by adopting the average uncertainties of the three model instances. The information entropy can then be calculated using $P\left(y_{i,j}\right) = m_{i,j}/\sum m_{i,j}$ and Eq. (5) with $m_{i,1} = 2$, $m_{i,2} = 0$ and $m_{i,3} = 1$.

Wang, Z. Z., Bertola, N. J., Goh, S. H., & Smith, I. F. C. (2021). Systematic selection of field response measurements for excavation back analysis. *Advanced Engineering Informatics*, *48*, 101296. https://doi.org/https://doi.org/10.1016/j.aei.2021.101296

The objectives of the analysis using the hierarchical algorithm are twofold. These are (i) the identification of the measurements within a selected inclinometer, or grouping of two or more inclinometers, that contribute to the information gain, and (ii) the identification of the inclinometers, either single or in groups, that provide the most information gain. To do so, the implementation of the hierarchical algorithm in this paper involves two steps, which will be explained with the aid of Figure 2.

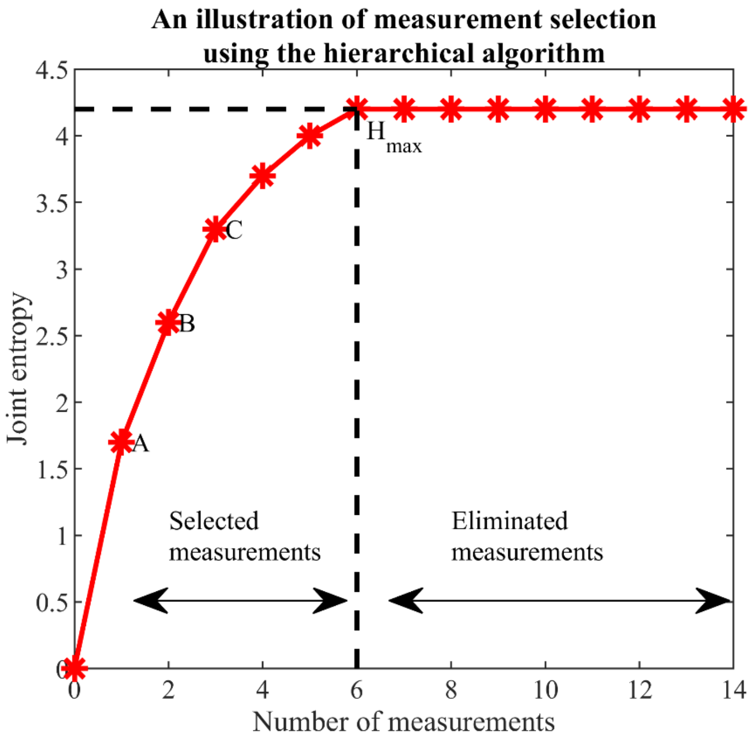

Figure 2 Measurement selection based on the measurement ranking using the hierarchical algorithm.

Step 1: The hierarchical algorithm is applied to all the measurements along a selected inclinometer. Joint entropies are first calculated using Eq. (5) for individual measurements, from which the measurements can be ranked in terms of the useful information yielded. Data point A in Figure 2 shows that the highest entropy value of 1.7 is computed among the individual measurements along the inclinometer. The particular measurement yielding the highest entropy is then adopted for subsequent joint entropy calculations involving

Wang, Z. Z., Bertola, N. J., Goh, S. H., & Smith, I. F. C. (2021). Systematic selection of field response measurements for excavation back analysis. *Advanced Engineering Informatics*, *48*, 101296. https://doi.org/https://doi.org/10.1016/j.aei.2021.101296

two or more measurements. Point B shows that, by combining the data from the highest entropy measurement with any other measurement along the inclinometer, the computed highest joint entropy using Eq. (6) for a grouping of two measurements is 2.6. When considering a grouping of three measurements that include the two measurements associated with data point B of Figure 2, the computed highest joint entropy is 3.4, as represented by Point C. Such a 'greedy search' technique can be extended to calculate the highest joint entropies associated with groupings of four or more measurements, as shown on Figure 2 for groupings of up to 12 measurements along the inclinometer. Figure 2 shows that the computed joint entropy increases with the number of measurements, albeit at a decreasing rate, such that it converges to a maximum value H_{max} after 6 measurements are used. The value H_{max} can be considered as a performance indicator which represents the maximum expected information gain achievable by the measurements along the selected inclinometer.

Step 2: The procedure outlined in Step 1 is repeated to compute the joint entropy response of all the inclinometers at the site. Besides considering individual inclinometers, the joint entropies are also evaluated for combined measurements obtained using groupings of two or more inclinometers. Hence, similar plots as that shown on Figure 2 can be generated for all other individual inclinometers, as well as groupings of two or more inclinometers. The joint entropy results from these analyses are used to rank the performance of the inclinometers and inclinometer groupings.

In summary, the information entropy, which measures the disorder in information content, evaluates the variability of model-instance predictions at measurement locations. A large entropy value corresponds to a high variability of model-instance predictions. Based on Eqs. (5) and (6), measurement location associated with a high variability of model-instance predictions is expected to falsify more model instances. This is in line with the concept of

Wang, Z. Z., Bertola, N. J., Goh, S. H., & Smith, I. F. C. (2021). Systematic selection of field response measurements for excavation back analysis. *Advanced Engineering Informatics*, *48*, 101296. https://doi.org/https://doi.org/10.1016/j.aei.2021.101296

model falsification wherein field measurement data that falsifies more model instances provide more information pertaining to material parameter values. Therefore, the information entropy provides a metric that can probabilistically quantify the performance of the model falsification exercise. By maximising the value of entropy, the hierarchical algorithm can identify the measurement data that provides the most information about the material parameter values.

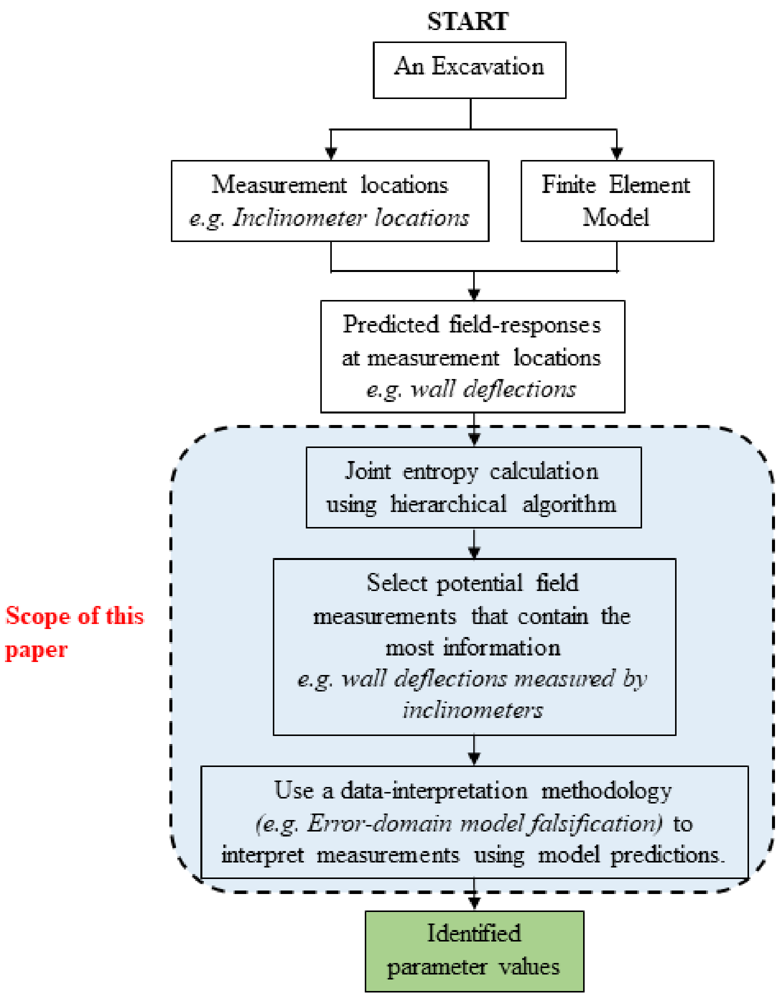

Figure 3 Proposed framework for geotechnical back analysis with systematic measurement selection algorithm.

Figure 3 shows how the methodologies in this section are integrated into a geotechnical back analysis. Before performing the back analysis with actual field measurement data, the hierarchical algorithm is first employed to identify field response measurements that maximise

Wang, Z. Z., Bertola, N. J., Goh, S. H., & Smith, I. F. C. (2021). Systematic selection of field response measurements for excavation back analysis. *Advanced Engineering Informatics*, *48*, 101296. https://doi.org/https://doi.org/10.1016/j.aei.2021.101296

the expected information gain, which will then be used to perform the back analysis. The framework described will be applied on an excavation case study in the following section.

3. Excavation Case Study

The geotechnical finite-element software package Plaxis 2D [5] and Plaxis 3D [3] are used to model the excavation and compute the wall deflection response. Deterministic finite element analysis that assumes homogenised properties within each soil layer is adopted. Although such an analysis does not consider the spatial variabilities of material properties, the use of a population-based data-interpretation methodology in the current study can account for, to some degree, the inherent variabilities of the material properties.

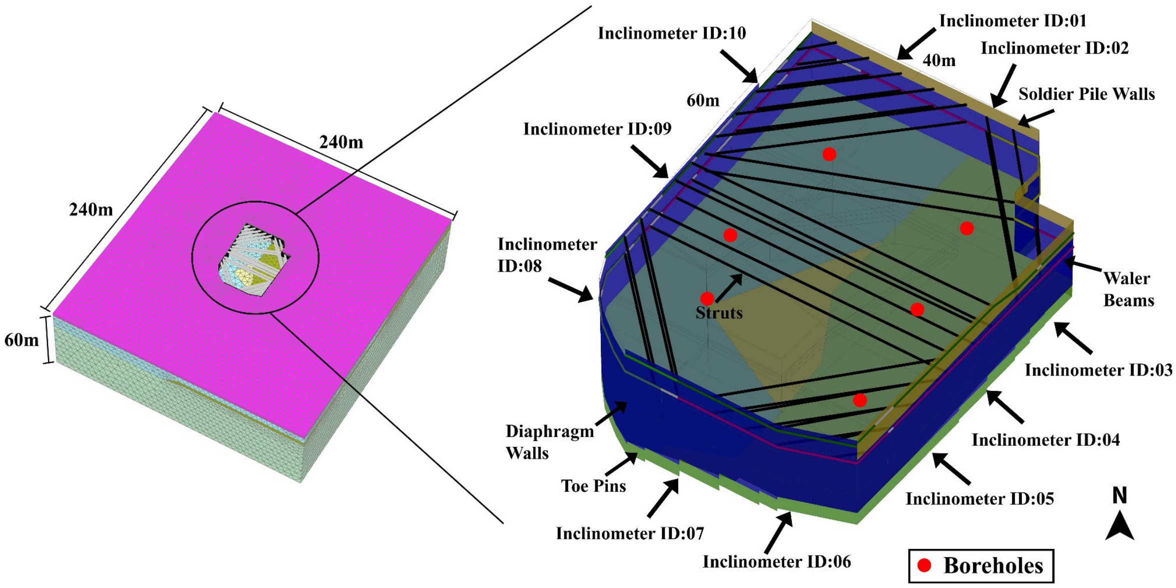

Figure 4 3D finite-element model of the excavation case study (with locations of all inclinometers shown).

The excavation is approximately 60 m in length, 40 m in width and 10 m in depth. The support system of the excavation includes diaphragm walls, soldier pile walls, toe pins and two layers of steel struts and waler beams. Figure 4 shows the 3D finite-element model of this project.

Wang, Z. Z., Bertola, N. J., Goh, S. H., & Smith, I. F. C. (2021). Systematic selection of field response measurements for excavation back analysis. *Advanced Engineering Informatics*, *48*, 101296. https://doi.org/https://doi.org/10.1016/j.aei.2021.101296

The 800 mm thick diaphragm walls are modelled as elastic plate members with the presence of construction joints between the panels captured by releasing the rotational stiffness between the plates [7, 14, 55]. The toe pins and the soldier pile walls, as a simplification, are smeared and modelled as elastic plate members with equivalent properties. Struts and waler beams are modelled as node-to-node anchors and beam elements respectively. Interface elements with zero thickness [5] is used to model the soil-wall interactions. The properties of all structural elements are listed in Table 1.

Table 1 Properties of structural elements involved in the excavation case history (underlined cell indicates the initial range of the identified parameter).

	Diaphragm Walls	**Toe Pins**	**Soldier Pile Walls**	**Concrete Waler Beams Type 1/2/3**	**Steel Waler Beams Type 1/2**	**Struts**
Thickness (m)	0.8	-	**-**	-	-	-
***EA*(kN)**	2.0E7	18E6	-	1.7E7/3.2E7/2.48E7	4.0E6/1.3E7	8.0E6
***EI*(kNm^2)**	1.1E6	11E3	**(3000-10000)**	7.0E5/2.1E6/1.3E6	2.6E5/8.8E5	-
$L_{spacing}$ (m)	-	-	-	-	-	10

Six boreholes were drilled at this site, which is situated on the Bukit Timah Granite formation. The borelogs from the six boreholes were interpreted to obtain the following geological stratigraphy. The top layer, which is roughly 3 m thick, contains mostly sandy silt and man-made backfill materials. It is underlain by a 10 to 13 m thick residual soil layer of sandy silt, denoted as G(VI), across most parts of the project site. The granitic rock layer G(III) is present at approximately 15 m below the ground surface. On the eastern half of the project site, there is also a 5 m thick layer of coarse sand sandwiched between the G(VI) sandy silt and G(III) granitic rock. In addition, the soil investigation report indicates that a pocket of medium to coarse gravels is present at a localised area near the centre of the pit. The fill layer and the gravels are described using the Mohr-Coulomb model while the rock layer is described using the Hoek-Brown model.

Wang, Z. Z., Bertola, N. J., Goh, S. H., & Smith, I. F. C. (2021). Systematic selection of field response measurements for excavation back analysis. *Advanced Engineering Informatics*, *48*, 101296. https://doi.org/https://doi.org/10.1016/j.aei.2021.101296

Other soil layers are simulated using the Hardening Soil with Small Strain Stiffness (HS Small) model [2]. This excavation generally shows low deflection magnitudes and thus, the capture of the higher stiffness at low strain levels is important for realistic wall-deflection predictions. Many studies [25, 30, 53] have highlighted the importance of small strain stiffness in excavation analyses.

Table 2 Properties of geological materials involved in the excavation case history (underlined cell indicates the initial range of the identified parameter).

	Fill	**Gravel**	**Sandy Silt Residual Soil**	**Coarse Sand**	**Rock**
***E* (MPa)**	<u>(3-20)</u>	40	-	-	2.5E3
E_{50}^{ref}(MPa)	-	-	<u>(5-50)</u>	<u>(5-50)</u>	-
E_{oed}^{ref}(MPa)	-	-	$1.0 * E_{50}^{ref}$	$1.0 * E_{50}^{ref}$	-
E_{ur}^{ref}(MPa)	-	-	$3.0 * E_{50}^{ref}$	$3.0 * E_{50}^{ref}$	-
m	-	-	0.6	0.6	-
***c'* (kPa)**	0	0	10	0	-
φ'(o)	25	40	28	35	-
ψ(o)	0	0	0	0	-
$\Upsilon_{0.7}$	-	-	0.0001	0.0001	-
G_0^{ref}(MPa)	-	-	$2 * E_{ur}^{ref}$	$2 * E_{ur}^{ref}$	-
p^{ref}(MPa)	-	-	100	100	-
σci (MPa)	-	-	-	-	80
mi	-	-	-	-	32.7
GSI	-	-	-	-	65
D	-	-	-	-	0.7
R_{inter}	0.7	0.5	0.7	0.7	0.75

Based on the laboratory test results of similar ground conditions, information pertaining to the strength parameters can be obtained, and the derived values are consistent with the representative parameter values reported for the Bukit Timah formation [39, 42]. However, the published laboratory tests provided very limited information related to the soil moduli, and this has provided the motivation for selecting the soil moduli as the parameters to be identified in the back analysis exercise. The material parameter values in the current study are listed in Table 2, except for the underlined cells which indicate the parameter values to be identified.

Wang, Z. Z., Bertola, N. J., Goh, S. H., & Smith, I. F. C. (2021). Systematic selection of field response measurements for excavation back analysis. *Advanced Engineering Informatics*, *48*, 101296. https://doi.org/https://doi.org/10.1016/j.aei.2021.101296

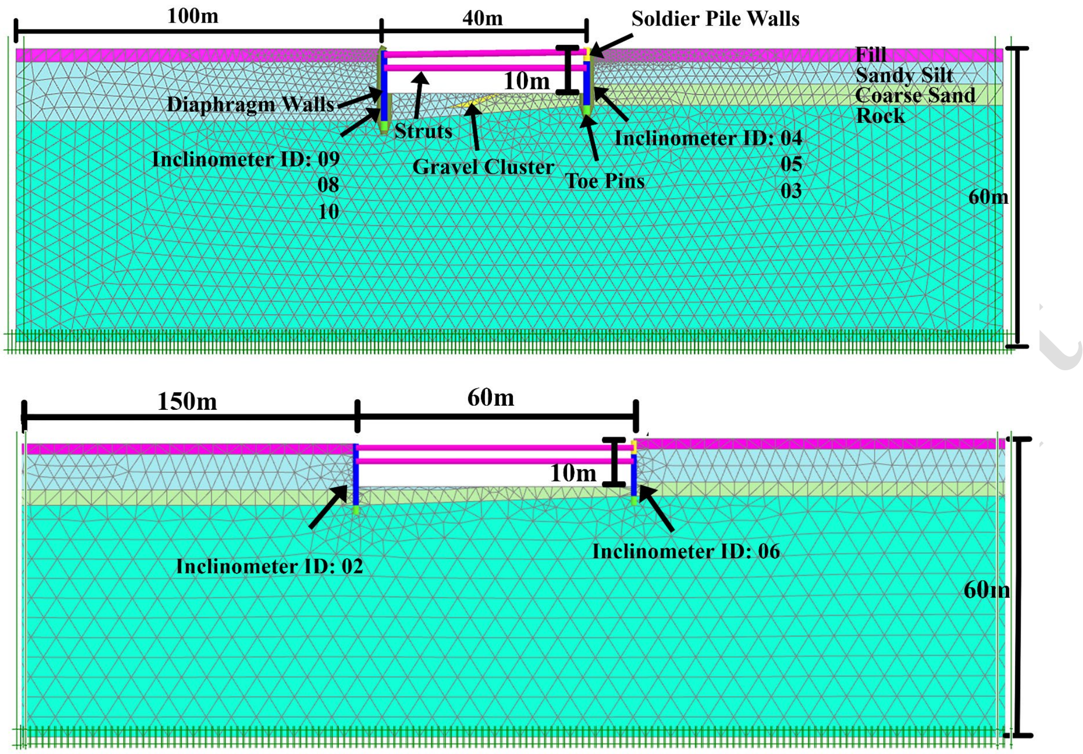

Figure 5 2D finite-element models of the excavation case study. Top: west-to-east section. Bottom: north-to-south section.

In the present study, two 2D finite-element models representing the east-to-west section and north-to-south section are built. The east-to-west model is used to simulate the behaviour of the diaphragm walls at the locations of inclinometers 3, 4, 5, 8, 9 and 10 while the north-to-south model is used to simulate the behaviour of the walls at the locations of inclinometers 2 and 6. Inclinometers 1 and 7 are excluded in the present study because they were reset in the field midway during the excavation activities. Figure 5 shows the two 2D finite-element models with the pertinent geological features, excavation support system and boundary conditions.

In this study, four parameters are selected for the identification exercise following a preliminary sensitivity analysis. These are (a) the Young's modulus E of the fill layer, (b) the reference Young's modulus E_{50}^{ref} of the G(VI) sandy silt layer, (c) the reference Young's modulus E_{50}^{ref} of the coarse sand layer and (d) the equivalent flexural rigidity EI of the smeared

Wang, Z. Z., Bertola, N. J., Goh, S. H., & Smith, I. F. C. (2021). Systematic selection of field response measurements for excavation back analysis. *Advanced Engineering Informatics*, *48*, 101296. https://doi.org/https://doi.org/10.1016/j.aei.2021.101296

soldier pile walls. Reasonable ranges of these parameter values at the start of the identification process, as indicated in the underlined cells of Tables 1 and 2, are estimated based on engineering judgement and local experience. Other Hardening Soil model reference moduli, such as E_{oed}^{ref}, E_{ur}^{ref} and G_0^{ref}, of the sandy silt and coarse sand layers are indirectly considered in the identification process via correlations to E_{50}^{ref}, as shown in the tables. Representative values for the Buikit Timah formation [39, 42] are assigned to soil parameters that are not involved in the identification. The initial water table is 2 m below the ground level.

Table 3 Simplified excavation activities and remarks.

Stage	Simplified Excavation Activities	Duration (days)	Calculation Type
0A	Initial Condition	-	Gravity Loading
0B	Wall Installation	-	Plastic
1	Excavate below Strut layer 1	20	Fully coupled flow-deformation
2	Install Strut layer 1	45	Fully coupled flow-deformation
3	Excavate below Strut layer 2	20	Fully coupled flow-deformation
4	Install Strut layer 2 and Excavate to formation level	30	Fully coupled flow-deformation

The construction sequence modelled in the finite element analysis comprises 6 stages, as shown in Table 3. As the interpreted soil layers are inclined with varying thicknesses, the initial ground stresses in stage 0A are generated using the gravity turn-on approach. The diaphragm wall is 'wished-in-place' in stage 0B, assuming negligible installation effects. Fully coupled flow-deformation calculations [10] are performed to account for the combined effects of groundwater flow and time-dependent consolidation.

The computations of the hierarchical algorithm and the back analyses are carried out with the help of response surfaces, these being constructed using the Gaussian process regression model [38] with 136 samples of the four parameter values to be identified. The performance of the response surfaces are validated using an additional 50 samples of the four parameters that are

Wang, Z. Z., Bertola, N. J., Goh, S. H., & Smith, I. F. C. (2021). Systematic selection of field response measurements for excavation back analysis. *Advanced Engineering Informatics*, *48*, 101296. https://doi.org/https://doi.org/10.1016/j.aei.2021.101296

not involved in their construction. The validated response surfaces are used as surrogates of the 2D finite element models shown in Figure 5 to make wall deflection predictions.

Figure 4 shows that some inclinometers are located near the excavation corners. Due to corner constraint effects, the wall deflections at these locations may not be properly captured using the 2D plane strain models. In this regard, the approach proposed by Wang et al. [50] can be used to quantify three-dimensional effects so that inclinometers near to excavation corners can be analysed in an efficient and accurate manner. This technique quantifies and represents the three-dimensional effects as uncertainty error terms, which are then subtracted from the predictions made with the 2D finite element models to arrive at the equivalent 3D predictions. The concept of correcting 2D model predictions to account for three-dimensional effects has been commonly adopted in the literature [9, 17, 22, 29]. The strategy used in the current study has been successfully applied on a synthetic excavation example [49] and two full-scale multi-stage excavation case histories in Singapore [51, 52].

Table 4 Examples of uncertainties used in the study.

Uncertainty sources	**Magnitudes**	**Remarks**
Inclinometer uncertainties	e.g. ±3.5mm	[8]
2D-model simplification	e.g. 0.9mm – 2.3mm	Quantified using approach in [51]
Response surface	e.g. ±2.5mm	-
Mesh refinement	±5%	[13 ,37]
Others	±5%	[13 ,37]

Table 4 lists the uncertainties involved in the analysis and their magnitudes. These uncertainty sources include inclinometer errors, 2D model simplification and errors arising from the use of response surfaces, among others. Uncertainties such as inclinometer errors and 2D model simplification can be quantified with reference to [8, 51], and these uncertainties vary across inclinometer locations and measurement points. The values shown in Table 4 are some selected values of such uncertainties.

4. Measurement Selection with the Hierarchical Algorithm

4.1. Individual inclinometer

The current study involves four excavation stages at which parameter identification is performed. It is often useful, at an early or intermediate point in the excavation process, to predict the field responses of subsequent excavation stages. Hence, a back analysis can be performed after every excavation stage. In the subsequent part of the paper, the term '1st round of identification' refers to the back analysis performed after excavation Stage 1, where wall deflection measurements of excavation stage 1 are used. Similarly, the term '4th round of identification' refers to the back analysis performed after excavation Stage 4, where wall deflection measurements of excavation Stages 1 to 4 are used. Therefore, the eight inclinometers are analysed four times corresponding to the four rounds of identification.

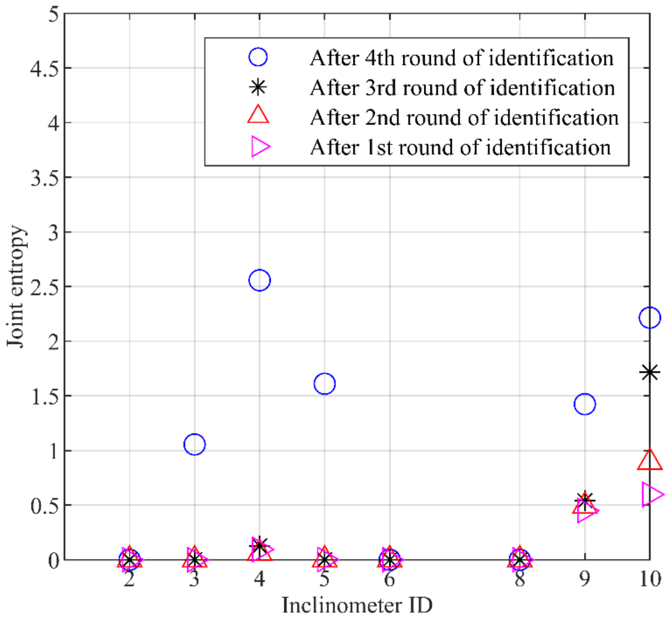

Figure 6 Joint entropy of eight inclinometers after each round of identification.

Figure 6 shows the joint entropy of the eight inclinometers after each round of identification. The joint entropy refers to the converged value after sufficient measurements along the inclinometer have been adopted in the hierarchical algorithmic calculations, as shown in Figure

Wang, Z. Z., Bertola, N. J., Goh, S. H., & Smith, I. F. C. (2021). Systematic selection of field response measurements for excavation back analysis. *Advanced Engineering Informatics*, *48*, 101296. https://doi.org/https://doi.org/10.1016/j.aei.2021.101296

2. In the current study, the joint entropy value is the metric that represents the expected knowledge about the material parameter values the inclinometer can provide. Figure 6 shows that inclinometers provide little information during the first three rounds of identification. This is because wall deflection magnitudes are small in the early excavation stages and hence are relatively insensitive to variations in parameter values. As the excavation proceeds to the final excavation stage, the deflection magnitudes become larger and more inclinometers are able to provide useful information.

Based on the joint entropy evaluations after the 4th round of identification, the five inclinometers, ranked in the order of 4, 10, 5, 9 and 3, are deemed to provide useful information. Therefore, the subsequent analyses will utilize wall deflection measurements of only inclinometers 4, 10, 5, 9 and 3 from all four excavation stages (after the 4th round of identification) because only these inclinometers and the associated measurements can potentially provide useful information about the material parameter values.

The objective of the current work is to demonstrate the effectiveness of the hierarchical algorithm in selecting field response measurements that maximise the expected information about the material parameter values that can be obtained from a back analysis. This may be done through a comparison between the results of the hierarchical algorithm and the back analyses after the 4th round of identification.

For the selected individual inclinometers, Figure 7 (a) plots the convergence of joint entropy with the number of measurements after the 4th round of identification. In this study, there is a distinction between a 'measurement' and a 'measurement point'. Each inclinometer contains between 11 to 15 measurement points that measure the lateral deflections at different depths to generate the wall deflection profile. As there are four stages in the excavation, each inclinometer will record four deflection profiles. This generates four measurements per measurement point, or a total of between 44 to 60 measurements per inclinometer for back analysis during the 4th round of identification.

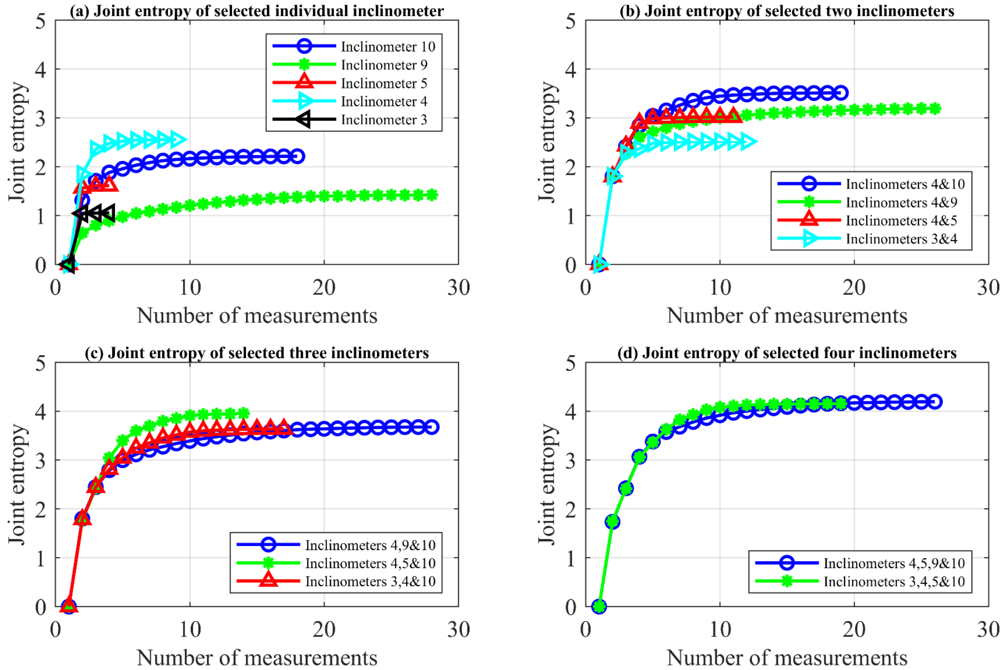

Figure 7 Convergence of joint entropy with respect to measurements for selected inclinometers and inclinometer groupings.

For the five inclinometers shown in Figure 7 (a), the individual joint entropies converge before all available measurements are included in the calculations, thus indicating that only a fraction of the 44 to 60 measurements recorded by each inclinometer is expected to provide useful information about the material parameter values. For example, only 8 measurements out of the 50 measurements recorded by inclinometer 4 provide useful information. Table 6 shows the information pertaining to these useful measurements for the selected five individual inclinometers. The numbers in the table indicate the depth the measurements are recorded. Studies related to the information provided by Table 6 will be presented in the later part of this paper.

Wang, Z. Z., Bertola, N. J., Goh, S. H., & Smith, I. F. C. (2021). Systematic selection of field response measurements for excavation back analysis. *Advanced Engineering Informatics*, *48*, 101296. https://doi.org/https://doi.org/10.1016/j.aei.2021.101296

Based on Figure 7(a), inclinometer 4 yields the highest joint entropy value, indicating that a back analysis that utilises measurement data of inclinometer 4 is likely to yield better knowledge about the material parameter values than the back analyses that utilise other individual inclinometers.

4.2. Joint entropy for inclinometer groupings

While the preceding section presents the expected information gain about the material parameter values when the selected inclinometers are used in a back analysis individually, the hierarchical algorithm is also able to analyse the expected information gain when combined measurement data of multiple inclinometers are utilised in the back analysis.

Table 5 Inclinometer groupings considered in the present study.

Single inclinometer	**Grouping of two inclinometers**	**Grouping of three inclinometers**	**Grouping of four inclinometers**	**Grouping of five inclinometers**
3; 4; 5; 9; 10	3&4; 4&5; 4&9; 4&10	3,4,&10; 4,5&10; 4,9&10	3,4,5,&10; 4,5,9&10	3,4,5,9&10

Table 6 Measurements that provide useful information (the numbers in the parenthesis indicate the depth the measurements are recorded).

Inclinometer ID	**Measurements (depth (m))**			
	Stage 1	**Stage 2**	**Stage 3**	**Stage 4**
3	-	-	-	1, 2
4	-	1	2, 4	1, 2, 3, 4, 5
5	-	-	-	1, 2, 3
9	1, 2, 3, 6	3, 4, 5, 6	2, 7, 8, 10	2, 3, 4, 5, 6, 7, 8, 9, 10, 11, 12, 13, 14
10	1, 3, 15	1, 2, 15	1, 15	1, 2, 3, 4, 5, 6, 7

Table 5 summarises the 15 inclinometer groupings that are considered in the present study. Using the greedy search approach in the hierarchical algorithm, it is not necessary to evaluate all possible combinations. For example, when groupings of two inclinometers are examined, inclinometer 4, which is the best individual inclinometer, is always included. Similarly, inclinometers 4 and 10, being the best grouping of two inclinometers (as will be shown in

Wang, Z. Z., Bertola, N. J., Goh, S. H., & Smith, I. F. C. (2021). Systematic selection of field response measurements for excavation back analysis. *Advanced Engineering Informatics*, *48*, 101296. https://doi.org/https://doi.org/10.1016/j.aei.2021.101296

Figure 7(b)), are always considered for the analysis that involves a grouping of three or more inclinometers.

Figures 7(b) to (d) plot the increase in the computed joint entropy values with the number of measurements associated with groupings of two to four inclinometers, after the 4th round of identification. As was noted earlier in Figure 7(a) for individual inclinometers, the joint entropy values calculated using measurements from the selected groupings of inclinometers also converge before all available measurements are taken into account. This again suggests that a significant fraction of the total measurements provide redundant information.

In Figure 7(b), the combination of inclinometers 4 and 10, which are the two 'best' inclinometers according to the converged joint entropy values of Figure 7(a), produces the largest joint-entropy value of approximately 3.5. In Figure 7(c), the grouping of inclinometers 4, 5 and 10, comprising the three 'best' individual inclinometers of Figure 7(a), provide the most information when measurements from three inclinometers are used simultaneously. Similarly, in Figure 7(d), the two cases involving four inclinometers (4, 5, 10 & 9; 4, 5, 10 & 3) yield similar joint-entropy values that are only marginally larger than the joint entropy value of the three-inclinometer grouping 4, 5 and 10.

Wang, Z. Z., Bertola, N. J., Goh, S. H., & Smith, I. F. C. (2021). Systematic selection of field response measurements for excavation back analysis. *Advanced Engineering Informatics*, *48*, 101296. https://doi.org/https://doi.org/10.1016/j.aei.2021.101296

Figure 8 plots the maximum joint entropy for different inclinometer groupings as a function of the number of inclinometers used. The individual joint entropy of inclinometer 4 is approximately 2.5. When two inclinometers are used, the joint entropy increases to 3.5 with the inclusion of inclinometer 10. However, when more inclinometers are considered, there are diminishing incremental gains in the joint entropy. Furthermore, when measurements from inclinometers 2, 6 or 8 (which are not useful inclinometers according to Figure 6) are included in the calculations, the computed value of joint entropy decreases. This demonstrates that it is not always favourable to include more field response measurement data.

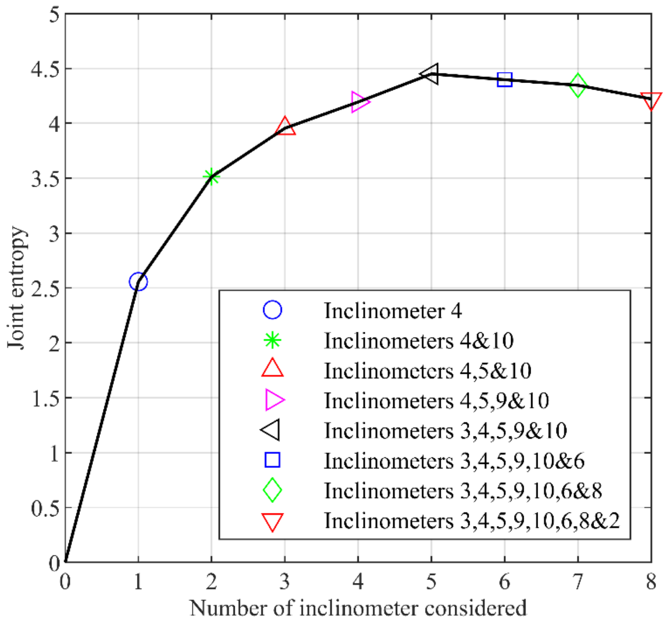

Figure 8 Maximum joint entropy values of different groupings of inclinometers.

5. Back Analysis with Field Measurement Data

In this section, the performance of the hierarchical algorithm in identifying and ranking the useful inclinometers is checked against the results from back analyses utilizing actual field measurements from different individual and selected groupings of the eight inclinometers.

Wang, Z. Z., Bertola, N. J., Goh, S. H., & Smith, I. F. C. (2021). Systematic selection of field response measurements for excavation back analysis. *Advanced Engineering Informatics*, *48*, 101296. https://doi.org/https://doi.org/10.1016/j.aei.2021.101296

In the introductory section of this paper, it was mentioned that the information entropy measures the "amount of information" contained in an event, and this information was loosely defined as the knowledge of the material parameter values and excavation behaviour. In the subsequent discussions, this "knowledge" refers to three aspects of the back analysis results: (i) the percentage of falsified models following the concept of EDMF, (ii) the range of the identified material parameter values and (iii) the standard deviations of the predicted wall deflections.

The results of the back analyses are first interpreted in terms of the percentage of material parameter values falsified during the EDMF process. The larger the falsification percentage, the smaller is the identified candidate set, which translates into a 'better' performance (in terms of information yield) of the particular individual or grouping of inclinometers from which the subset of field measurements is utilized in the back analysis. Hence, the use of the falsification percentage as a performance metric is reasonable and compatible with the approach adopted by [12]. Similarly, a smaller range of the identified material parameter values and a smaller standard deviation of the predicted wall deflections also translate into a "better" performance.

The back analyses are performed by first generating 20,000 initial samples of the four material parameters to be identified using the Latin Hypercube sampling technique, for which the corresponding wall deflection predictions are obtained using response surfaces derived from finite-element simulations. The error-domain model falsification (EDMF) method is then adopted to identify the parameter candidate sets by comparing the predicted wall deflections with field measurements. Different back analyses are performed by using field measurements from different individual and groupings of inclinometers, each of which will result in a different identified candidate set.

Following the above methodology, back analyses are performed using field measurements from individual inclinometer and groupings of two to five inclinometers, as listed in Table 5.

Wang, Z. Z., Bertola, N. J., Goh, S. H., & Smith, I. F. C. (2021). Systematic selection of field response measurements for excavation back analysis. *Advanced Engineering Informatics*, *48*, 101296. https://doi.org/https://doi.org/10.1016/j.aei.2021.101296

First, back analyses using all measurements obtained from either individual inclinometers or groupings of inclinometers are carried out. The results are interpreted in terms of percentage falsification for individual inclinometers or inclinometer groupings, which can then be compared with the rankings of inclinometers and inclinometer groupings presented in Section 4 using the hierarchical algorithm. Second, back analyses are performed using EDMF with only the selected measurement subsets, such as those measurements listed in Table 6, from individual inclinometers or inclinometer groupings.

5.1. Percentage of falsified models

5.1.1. Using all measurements from individual inclinometers and inclinometer groupings

Figure 9(a) shows the percentage of falsified models obtained by using field measurements from the individual inclinometers. The individual inclinometer that produces the highest percentage of falsified model is inclinometer 4, which may also be interpreted as the instrument yielding the most information about the material parameter values. This agrees with the assessment of the expected information gain obtained from the hierarchical algorithm discussed in Section 4. Both the back analyses and the hierarchical algorithm indicate that the next two best individual inclinometers are inclinometers 10 and 5; however, the back analysis shows that the use of measurements from inclinometer 5 produces a slightly higher percentage of falsified models compared to inclinometer 10, which is contrary to the joint entropy results of the hierarchical algorithm. For inclinometers 9 and 3, the results of the back analyses are in agreement with the hierarchical-algorithm results.

Figure 9(b) to (e) shows the percentage of falsified models using the field measurements associated with groupings of two or more inclinometers. Globally, the results of the back analyses, in terms of the inclinometer falsification performance, are in agreement with the joint

Wang, Z. Z., Bertola, N. J., Goh, S. H., & Smith, I. F. C. (2021). Systematic selection of field response measurements for excavation back analysis. *Advanced Engineering Informatics*, *48*, 101296. https://doi.org/https://doi.org/10.1016/j.aei.2021.101296

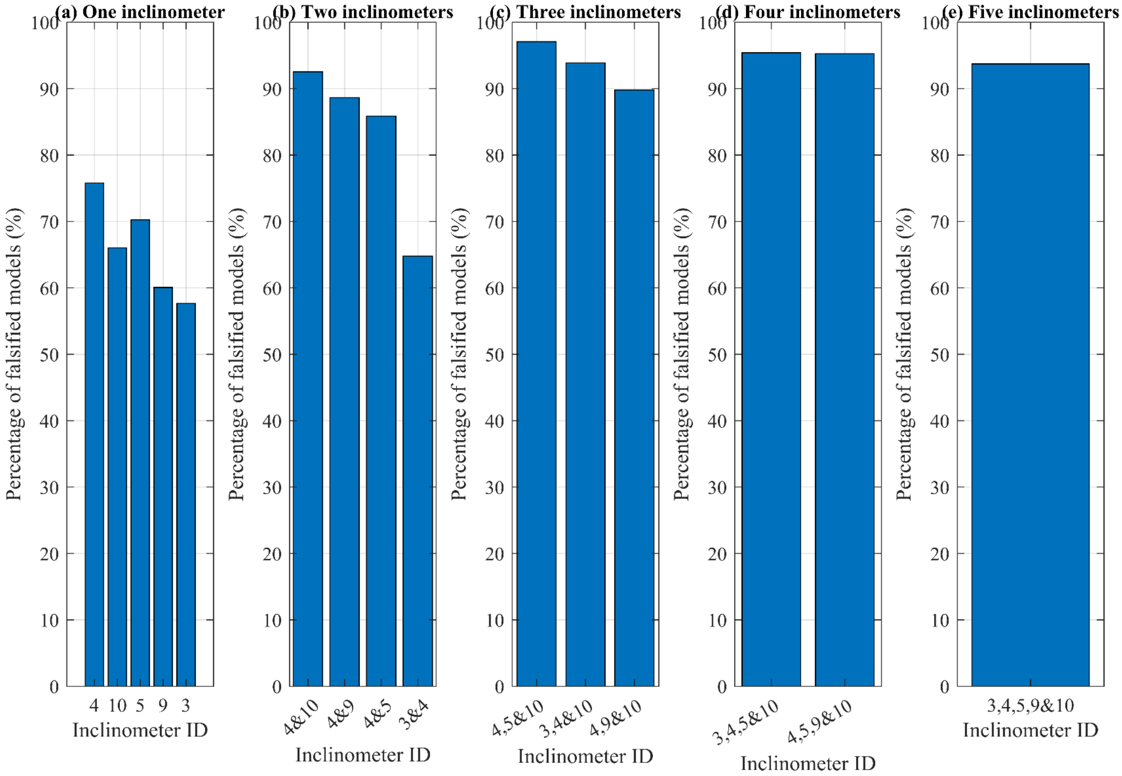

Figure 9 Percentage of falsified models for groupings of one or more inclinometers.

entropy calculations of the hierarchical algorithm. The grouping of inclinometers 4 and 10 yields the highest percentage of falsified models among all groupings of two inclinometers, which is consistent with the results of the hierarchical algorithm in Figure 7 (b). The rankings of the other three groupings of two inclinometers also agree well with that of the hierarchical algorithm. For groupings of three inclinometers, both the back analyses and the hierarchical algorithm show that the grouping of inclinometers 4, 5 and 10 yields the most information. The back analyses also show that the grouping of inclinometers 3, 4, 5, and 10 offers similar performance as the inclinometer grouping 4, 5, 9 and 10, which is consistent with the outcome using the hierarchical algorithm in Figure 7(d).

Figure 10 plots, for each grouping of inclinometers, the highest percentage of falsified models within that group. Both Figures 8 and 10 illustrates a possible adverse effect of including too much measurement data [12], as can be seen in the small drop in the value of joint entropy and

Wang, Z. Z., Bertola, N. J., Goh, S. H., & Smith, I. F. C. (2021). Systematic selection of field response measurements for excavation back analysis. *Advanced Engineering Informatics*, *48*, 101296. https://doi.org/https://doi.org/10.1016/j.aei.2021.101296

the percentage of falsified model instances. However, in contrast to Figure 8, which indicates that additional information can be gained with the inclusion of more data taken from up to five inclinometers (using the hierarchical algorithm), Figure 10 shows that no further information gain is achieved by using measurements from more than three inclinometers (from the back analysis exercise). This discrepancy is possibly due to the probabilistic nature of the hierarchical algorithm and simplifications adopted in the evaluation of the joint entropy (see Section 2.2).

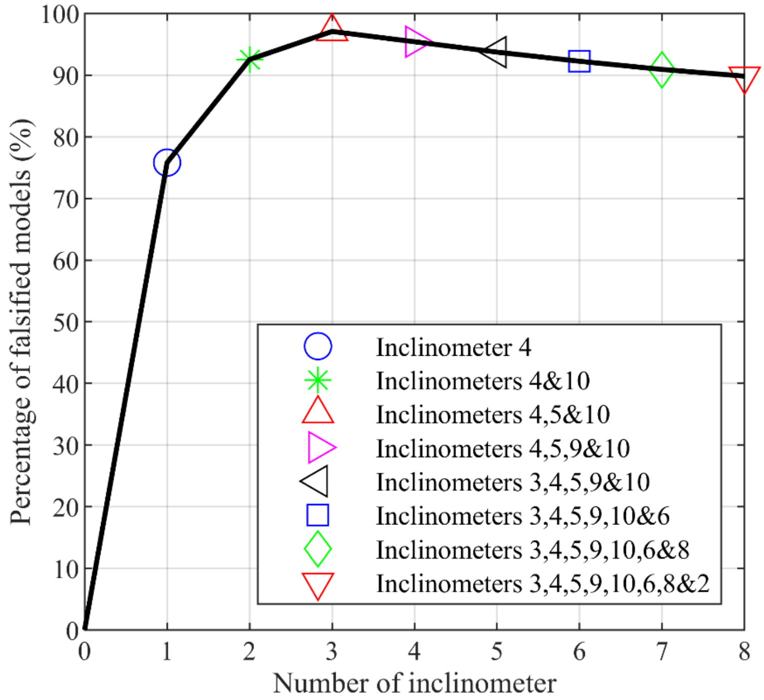

Figure 10 Maximum percentage of falsified models for various inclinometer groupings.

5.1.2. Using only selected measurements from individual inclinometers and groupings

As indicated in Figure 7(a) to (d), not all measurements associated with each inclinometer deflection profile provide useful information. Therefore, the measurements that do not belong to the subset of measurements selected by the hierarchical algorithm are not considered to be "useful" for the back analysis. In the subsequent analysis, back analyses are performed using just this subset of measurements (Table 6) that are considered to be "useful" by the hierarchical

Wang, Z. Z., Bertola, N. J., Goh, S. H., & Smith, I. F. C. (2021). Systematic selection of field response measurements for excavation back analysis. *Advanced Engineering Informatics*, *48*, 101296. https://doi.org/https://doi.org/10.1016/j.aei.2021.101296

algorithm in Section 4. Results are then compared against those from the preceding analyses that utilise all measurements.

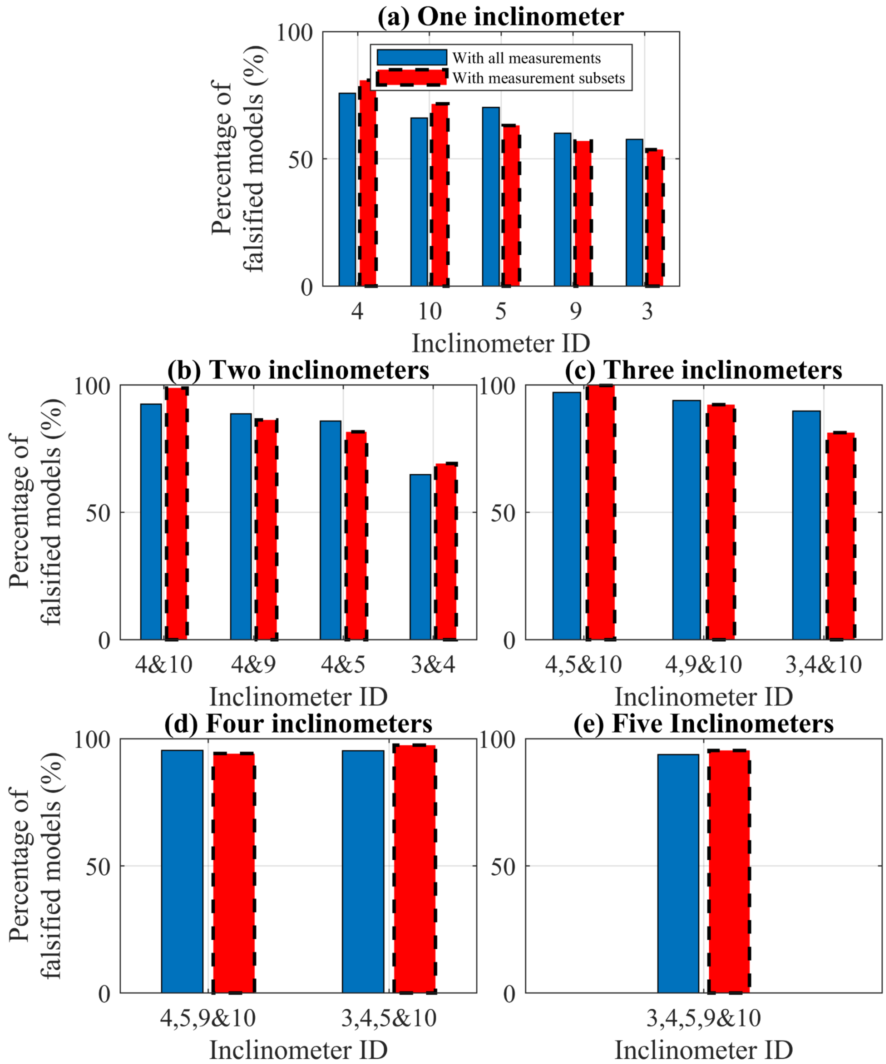

Figure 11 Percentage of falsified models of individual inclinometer and groupings of two to five inclinometers with all measurements or subsets of measurements.

Figure 11(a) compares the percentage of falsified models for the back analyses using the full sets versus the selected subsets of measurements from individual inclinometers. The dashed red bars correspond to results obtained using the subset of measurements, while the solid bars are the results obtained utilizing all measurements. The close agreement in the percentage of falsified models for each inclinometer imply that generally similar information is obtained

Wang, Z. Z., Bertola, N. J., Goh, S. H., & Smith, I. F. C. (2021). Systematic selection of field response measurements for excavation back analysis. *Advanced Engineering Informatics*, *48*, 101296. https://doi.org/https://doi.org/10.1016/j.aei.2021.101296

using both the subset and the full set of measurements. In a similar manner to Figure 11(a), Figure 11(b) to (e) compares the percentage of falsified models for the back analyses using the full sets versus the selected subsets of measurements by the hierarchical algorithm for groupings of two to five inclinometers. The analyses that use all measurements (indicated by solid bars) do not yield significant variations in the percentages of falsified models when compared with the analyses using subsets of measurements selected by the hierarchical algorithm (indicated by bars with dashed outlines). These observations corroborate the selection obtained using the hierarchical algorithm, and suggest that the hierarchical algorithm is effective in identifying the measurements that provide useful information about the parameter values in a back analysis.

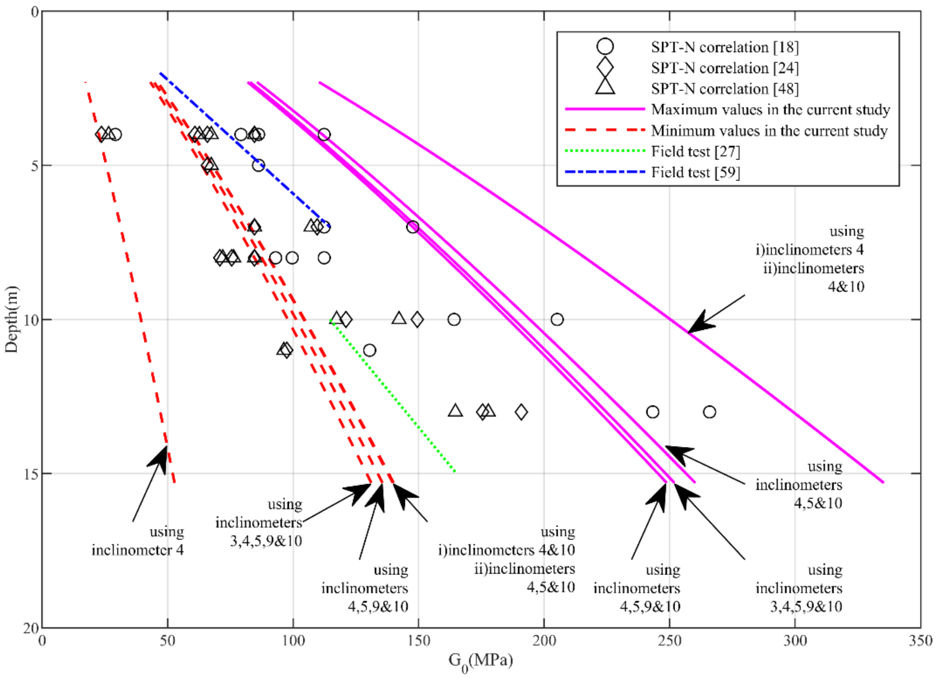

Figure 12 Comparisons of identified values of small strain stiffness G_0 (MPa) of sandy silt using different individual and grouping of inclinometers with reference values reported in the literature [18, 24, 27, 48, 59].

Wang, Z. Z., Bertola, N. J., Goh, S. H., & Smith, I. F. C. (2021). Systematic selection of field response measurements for excavation back analysis. *Advanced Engineering Informatics*, *48*, 101296. https://doi.org/https://doi.org/10.1016/j.aei.2021.101296

5.2. Identified material parameter values

Given that the excavation in this case study exhibits fairly small deflection magnitudes (as will be shown in Figure 13) and that the sandy silt layer is the dominant geological material, the identified values of the small strain stiffness G_0 are chosen for subsequent discussions. As indicated in Table 2, the values of G_0^{ref} are correlated to the values of E_{50}^{ref} [1]. Values of G_0 can then be calculated based on the identified values of G_0^{ref} and the effective minor principal stress extracted from the finite element analysis following the equation described in [3, 5].

Figure 12 compares the identified values of G_0 with values obtained from (i) correlations with SPT-N values [18, 24, 48] and (ii) geophysical tests on similar grounds [27, 59]. Multiple lines that correspond to the maximum and minimum values of G_0 identified using different field response measurements are shown in the figure. These values correspond to the candidates separately obtained from the back analyses using measurements of (i) inclinometer 4, (ii) grouping of inclinometers 4 and 10, (iii) grouping of inclinometers 4, 5 and 10, (iv) grouping of inclinometers 4, 5, 9 and 10, and (v) (ii) grouping of inclinometers 3, 4, 5, 9 and 10. These individual inclinometers and groupings of inclinometers are selected based on the results shown in Figure 8. The key observations are summarised as follows:

(i) The G_0 values calculated using correlations to in-situ SPT-N values [18, 24, 27, 48, 59] are reasonably bounded by the maximum and minimum values obtained from all the five back analyses using different combinations of the inclinometers. This comparison supports the claim that the back analyses carried out are reliable and have led to reasonable identification of the material parameter values.

(ii) The back analysis carried out using measurements of inclinometer 4 yields the widest bounds of G_0 values. While the use of combined measurements of inclinometers 4 and 10 effectively reduces the bounds of G_0 values obtained from the preceding case, the use of combined measurements of inclinometers 4, 5 and 10 further reduces the bounds of

Wang, Z. Z., Bertola, N. J., Goh, S. H., & Smith, I. F. C. (2021). Systematic selection of field response measurements for excavation back analysis. *Advanced Engineering Informatics*, *48*, 101296. https://doi.org/https://doi.org/10.1016/j.aei.2021.101296

G_0 values. However, the reduction in the G_0 bounds achieved by inclinometers 4, 5 and 10 is less than the reduction achieved by inclinometers 4 and 10. Moreover, minor variations in the maximum and minimum values are observed when additional measurements from inclinometers 3 and 9 are included in the back analysis.

Observation (ii) implies that while improved knowledge about the material parameter values, in the form of a narrower bound, can be obtained by using more measurements in the back analyses, the improvement is not proportionate to the quantity of the measurements. Eventually, the information gain attains a plateau and therefore, the strategy to use as much measurement data as possible in the back analysis may not necessarily be effective in gaining the maximum knowledge about the parameter values. Such a conclusion is consistent with that drawn from Figures 8 and 10, which respectively show the improvements in joint entropy and percentage of falsified models diminish with the inclusion of additional measurement data.

5.3. Wall-deflection predictions

Figure 13 shows the wall deflection predictions at the locations of the five selected inclinometers (3, 4, 5, 9 and 10) made with material parameter values identified from the back analysis using combined measurements of inclinometers 4, 5 and 10, which yields the best knowledge of the material parameter values based on Figures 10 and 12. As explained in Section 2.1, EDMF is a population-based approach that identifies a population of candidate material parameter values. All candidate parameter values are then used to produce a population of wall deflection predictions. Both mean predictions and 95% confidence bounds are calculated based on this population of predictions and are shown in the Figure 13. Good agreement between measurements and predictions is observed for all five inclinometers, implying that the back analyses carried out are reliable and have led to reasonably accurate predictions of wall deflections.

Wang, Z. Z., Bertola, N. J., Goh, S. H., & Smith, I. F. C. (2021). Systematic selection of field response measurements for excavation back analysis. *Advanced Engineering Informatics*, *48*, 101296. https://doi.org/https://doi.org/10.1016/j.aei.2021.101296

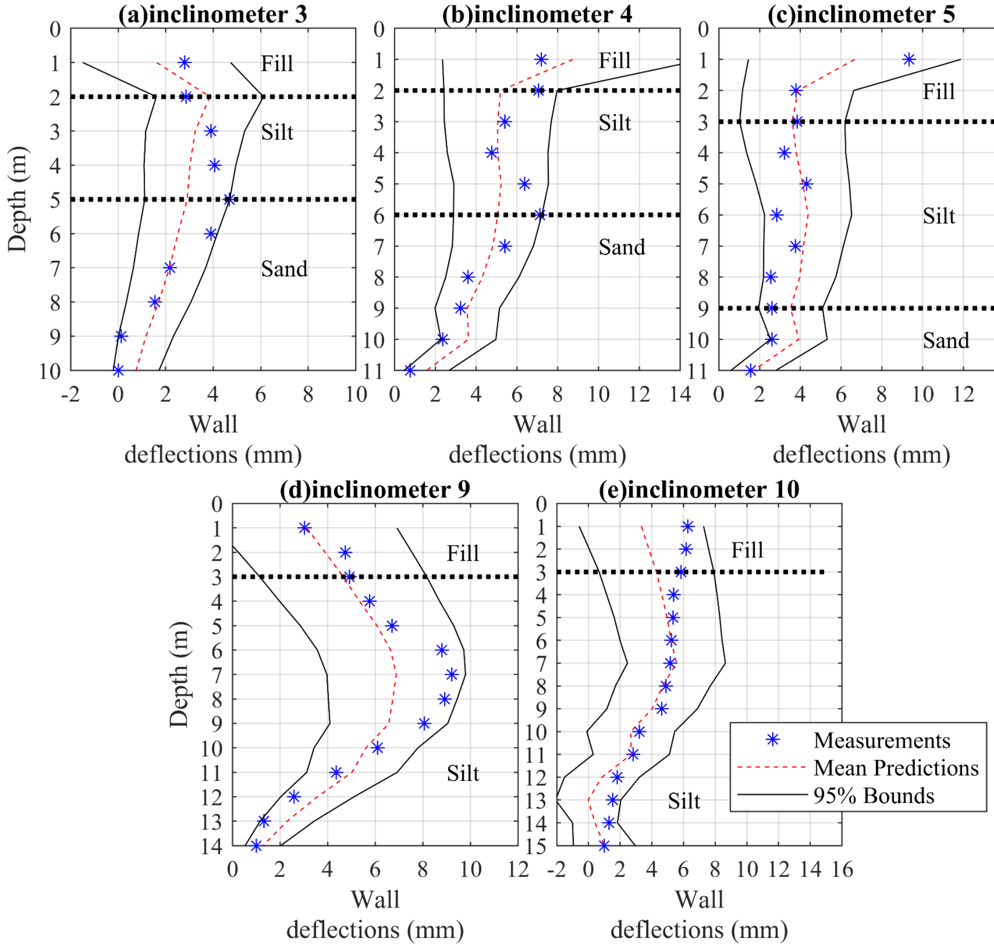

Figure 13 Wall deflection predictions at locations of the five selected inclinometers made at excavation stage 4 with material parameter values identified using combined all measurements of inclinometers 4, 5 and 10.

Figure 14 shows the 'averaged' standard deviations of wall deflection predictions at the locations of the five selected inclinometers (3, 4, 5, 9 and 10) made at excavation stage 4 with material parameter values identified using combined measurements of several groupings of inclinometers. These 'averaged' standard deviations are obtained by evaluating the mean values of the standard deviations calculated for all the measurements and stages of the individual inclinometer-measured wall deflection profile. This is done in an attempt to evaluate the overall variability of the predicted wall deflections across all measurement points and excavation stages.

Wang, Z. Z., Bertola, N. J., Goh, S. H., & Smith, I. F. C. (2021). Systematic selection of field response measurements for excavation back analysis. *Advanced Engineering Informatics*, *48*, 101296. https://doi.org/https://doi.org/10.1016/j.aei.2021.101296

In general, the use of combined measurements of inclinometers 4, 5 and 10 leads to the lowest values of standard deviations for all five inclinometers, implying that the wall deflection predictions in this case are the most precise. In addition, the standard deviations obtained using combined measurements of inclinometers 4, 5, 9 and 10 and inclinometers 3, 4, 5, 9, 10 are very similar to the values obtained using combined measurements of inclinometers 4, 5 and 10. These observations again suggest that the gain in knowledge of the excavation behaviour, as manifested in the form of narrower bounds of the predicted wall deflections, diminishes with additional measurements utilized in the back analysis. The inclusion of additional measurements beyond a certain quantity may not confer any improvements on the performance predictions. These observations are consistent with those presented in Figures 8, 10 and 12.

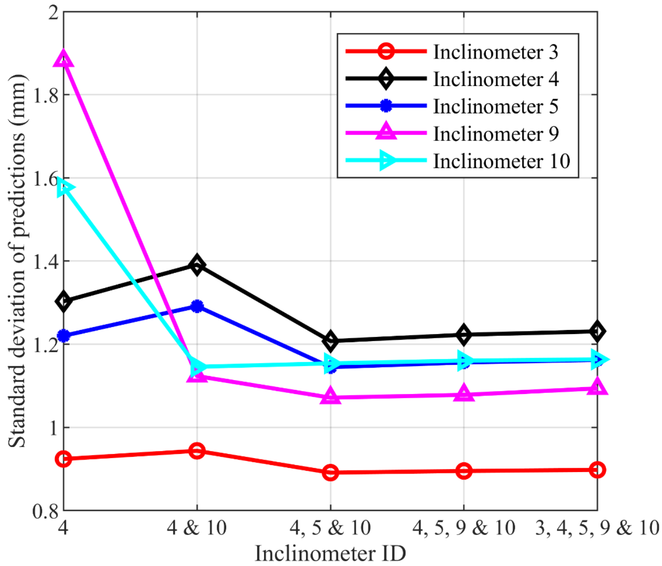

Figure 14 Standard deviations of wall deflection predictions at locations of the five selected inclinometers made at excavation stage 4 with material parameter values identified using combined measurements of grouping of inclinometers. (unit: mm)

6. Implications on Back Analysis of Excavations

Based on the common practice of performing excavation analyses using plane strain assumptions [8, 14, 15, 41], the measurements from inclinometers 4 and 9 will typically be chosen for routine back analysis. Engineering heuristics also suggest that inclinometer 9, which

Wang, Z. Z., Bertola, N. J., Goh, S. H., & Smith, I. F. C. (2021). Systematic selection of field response measurements for excavation back analysis. *Advanced Engineering Informatics*, *48*, 101296. https://doi.org/https://doi.org/10.1016/j.aei.2021.101296

records the largest deflection magnitudes (Figure 13), is likely to be the most useful inclinometer for a back analysis. Although the results from both the hierarchical algorithm and the back analyses (Figures 7 and 9) support the selection of inclinometers 4 and 9 as good sensors in general, they also indicate that inclinometers 5 and 10 are better choices than inclinometer 9. Inclinometer 9, which mainly penetrates through the sandy silt layer only as shown in Figure 13, likely contains useful information pertaining primarily to this layer. As a result, the usefulness of the information gained from this inclinometer would be more limited. In contrast, inclinometers 4 and 5, which measure responses pertaining to multiple geological members and structural members as shown in Figure 13, can provide more diverse and useful information.

When combined measurements of multiple inclinometers are to be used for a back analysis, it is recommended to have inclinometers that are not located on the same side of the excavation. In Figures 7(b) and 9(b), the best two-inclinometer combinations are the groupings of inclinometers 4 and 10 followed by 4 and 9. In both cases, the two inclinometers are located on opposite sides of the excavation. When combined measurements of three inclinometers are to be used, the best grouping is inclinometers 4, 5 and 10, in which inclinometers 5 and 10 are located diagonally across the site.

Furthermore, engineering heuristics often suggest that the use of measurement data of one inclinometer is often insufficient for getting the best knowledge about the material parameter values. While the current study supports this statement, it also shows that the use of combined measurements of two inclinometers (e.g. inclinometers 4 and 9), which is the typical strategy adopted in the literature [8, 15, 41], is not necessarily the optimal choice as shown in Figures 7 and 9.

It may be surmised from the above observations that, while considerations pertaining to plane strain assumption and deflection magnitudes are important, it is recommended to take diversity

Wang, Z. Z., Bertola, N. J., Goh, S. H., & Smith, I. F. C. (2021). Systematic selection of field response measurements for excavation back analysis. *Advanced Engineering Informatics*, *48*, 101296. https://doi.org/https://doi.org/10.1016/j.aei.2021.101296

of information into consideration when selecting field response measurements for a back analysis. The above observations also suggest that, while a selection based on engineering heuristics (e.g. inclinometers 4 and 9) can yield reasonable results, the rational and systematic selection and adoption of field response measurements collected at appropriate sensor locations is able to provide a more robust strategy to ensure maximum useful information gain from a back analysis.

7. Limitations and Conclusions

The following limitations of the work are recognized:

The combined uncertainties used in the hierarchical algorithm are calculated as the mean values of the uncertainties associated with the 1000 model instances to reduce computational effort. Such a simplification may inevitably influence the computational results, which may explain some of the observed discrepancies between the results of the hierarchical algorithm and the back analysis.

In addition, the greedy-search strategy used by the hierarchical algorithm does not automatically lead to a global optimum of the joint entropy, particularly for small numbers of measurements. Given that the results of the hierarchical algorithm are largely in agreement with the results of the back analysis, these limitations are likely to have little impact.

Furthermore, Figure 9 suggests that limited knowledge of the material parameter values is obtained during the first three rounds of identification. In this case study, wall deflection magnitudes are small in the early excavation stages, and hence are relatively insensitive to variations in parameter values. Consequently, the inclinometer measurements at early excavation stages provide limited information. This is a limitation specific to the inherent nature of this case study. Nevertheless, both the back analysis and the hierarchical algorithm produce similar inclinometer ranking after the fourth round of identification. This observation

Wang, Z. Z., Bertola, N. J., Goh, S. H., & Smith, I. F. C. (2021). Systematic selection of field response measurements for excavation back analysis. *Advanced Engineering Informatics*, *48*, 101296. https://doi.org/https://doi.org/10.1016/j.aei.2021.101296

lends support to the conclusion that the hierarchical algorithm is effective in selecting measurement data that allows good and useful knowledge of material parameter values to be obtained from a back analysis.

A limited number of settlement markers were installed for the current case history. Unfortunately, they could not be used due to the erroneous readings that were recorded. Additional case histories that involve both wall deflections and ground settlement measurements should be considered in future studies to further substantiate the effectiveness of the hierarchical algorithm.

In summary, this paper examines the effectiveness of the hierarchical algorithm as a tool to systematically select measurement data to maximise the information gain from a back analysis of an excavation. The application of the hierarchical algorithm does not entail the use of any actual measurements from the field excavation, and therefore, such an exercise can be carried out at an early stage of the project to help identify potential inclinometer measurements for back analysis. The results have been corroborated using a back analysis performed on an excavation case history in Singapore. Specific conclusions are summarised as follows:

(i) A hierarchical algorithm that is formulated based on joint-entropy values leads to effective evaluation of the mutual and redundant knowledge of material parameter values.

(ii) The hierarchical algorithm can serve as a tool for engineers to accurately identify and select measurements that provide the most useful knowledge of material parameter values in a back analysis exercise.

(iii) By comparing back analysis results using all inclinometer measurements and subsets of measurements, the performance of the hierarchical algorithm is validated using field response measurements.

Wang, Z. Z., Bertola, N. J., Goh, S. H., & Smith, I. F. C. (2021). Systematic selection of field response measurements for excavation back analysis. *Advanced Engineering Informatics*, *48*, 101296. https://doi.org/https://doi.org/10.1016/j.aei.2021.101296

Acknowledgments

This research was conducted at the Future Cities Laboratory at the Singapore-ETH Centre (SEC). The SEC was established as a collaboration between ETH Zurich and National Research Foundation (NRF) Singapore (FI 370074011) under the auspices of the NRF's Campus for Research Excellence and Technological Enterprise (CREATE) program.

References

[1] Alpan, I. (1970). The geotechnical properties of soils. *Earth Science Reviews*. https://doi.org/10.1016/0012-8252(70)90001-2

[2] Benz, T., Vermeer, P. A., & Schwab, R. (2009). A small-strain overlay model. *International Journal for Numerical and Analytical Methods in Geomechanics*. https://doi.org/10.1002/nag.701

[3] Brinkgreve, R. B. J., Engin, E., & Swolf, W. M. (2013). Plaxis 3d 2013. *Plaxis Bv*.

[4] Bertola, N. J., Papadopoulou, M., Vernay, D., & Smith, I. F. C. (2017). Optimal multi-type sensor placement for structural identification by static-load testing. *Sensors (Switzerland)*. https://doi.org/10.3390/s17122904

[5] Brinkgreve, R. B. J., Kumarswamy, S., Swolfs, W. M., Zampich, L., & Manoj, N. R. (2019). Plaxis 2D Reference Manual 2019. *Rotterdam, Netherlands, Balkema*.

[6] Bertola, N. J., Cinelli, M., Casset, S., Corrente, S., & Smith, I. F. C. (2019). A multi-criteria decision framework to support measurement-system design for bridge load testing. *Advanced Engineering Informatics*. https://doi.org/10.1016/j.aei.2019.01.004

[7] Dong, Y. P., Burd, H. J., & Houlsby, G. T. (2016). Finite-element analysis of a deep excavation case history. *Geotechnique*. https://doi.org/10.1680/jgeot.14.P.234

[8] Finno, R. J., & Calvello, M. (2005). Supported Excavations: Observational Method and Inverse Modeling. *Journal of Geotechnical and Geoenvironmental Engineering*. https://doi.org/10.1061/(ASCE)1090-0241(2005)131:7(826)

Wang, Z. Z., Bertola, N. J., Goh, S. H., & Smith, I. F. C. (2021). Systematic selection of field response measurements for excavation back analysis. *Advanced Engineering Informatics*, *48*, 101296. https://doi.org/https://doi.org/10.1016/j.aei.2021.101296

[9] Finno, R. J., Blackburn, J. T., & Roboski, J. F. (2007). Three-dimensional effects for supported excavations in clay. *Journal of Geotechnical and Geoenvironmental Engineering*. https://doi.org/10.1061/(ASCE)1090-0241(2007)133:1(30)

[10] Galavi, V. (2010). Groundwater flow, fully coupled flow deformation and undrained analyses in PLAXIS 2D and 3D. In *Plaxis Internal Report*. https://doi.org/j.1746-1561.2005.tb07343.x10.1111/j.1746-1561.2005.00038.x

[11] Goulet, J. A., Kripakaran, P., & Smith, I. F. C. (2010). Multimodel structural performance monitoring. *Journal of Structural Engineering*. https://doi.org/10.1061/(ASCE)ST.1943-541X.0000232

[12] Goulet, J.-A. (2012). Probabilistic Model Falsification for Infrastructure Diagnosis, Doctoral Thesis. In *Doctoral Thesis*.

[13] Goulet, J. A., & Smith, I. F. C. (2013). Performance-driven measurement system design for structural identification. *Journal of Computing in Civil Engineering*. https://doi.org/10.1061/(ASCE)CP.1943-5487.0000250

[14] Hashash, Y. M. A., Marulanda, C., Ghaboussi, J., & Jung, S. (2006). Novel approach to integration of numerical modeling and field observations for deep excavations. *Journal of Geotechnical and Geoenvironmental Engineering*. https://doi.org/10.1061/(ASCE)1090-0241(2006)132:8(1019)

[15] Hashash, Y. M. A., Levasseur, S., Osouli, A., Finno, R., & Malecot, Y. (2010). Comparison of two inverse analysis techniques for learning deep excavation response. *Computers and Geotechnics*. https://doi.org/10.1016/j.compgeo.2009.11.005

[16] Hashash, Y. M. A., Song, H., & Osouli, A. (2011). Three-dimensional inverse analyses of a deep excavation in Chicago clays. *International Journal for Numerical and Analytical Methods in Geomechanics*. https://doi.org/10.1002/nag.949

[17] Hsiung, B. C. B., Yang, K. H., Aila, W., & Hung, C. (2016). Three-dimensional effects of a deep excavation on wall deflections in loose to medium dense sands. *Computers and Geotechnics*, *80*, 138-151.

[18] Imai, T., & Tonouchi, K. (1982). Correlation of N value with S-wave velocity and shear modulus. *Penetration Testing. Proc. 2nd European Symposium, Amsterdam, 1982*.

Wang, Z. Z., Bertola, N. J., Goh, S. H., & Smith, I. F. C. (2021). Systematic selection of field response measurements for excavation back analysis. *Advanced Engineering Informatics*, *48*, 101296. https://doi.org/https://doi.org/10.1016/j.aei.2021.101296

[19] Ieronymaki, E., Whittle, A. J., & Einstein, H. H. (2018). Comparative study of the effects of three tunneling methods on ground movements in stiff clay. *Tunnelling and Underground Space Technology*. https://doi.org/10.1016/j.tust.2018.01.005

[20] Javadi, A. A., & Rezania, M. (2009). Intelligent finite element method: An evolutionary approach to constitutive modeling. *Advanced Engineering Informatics*. https://doi.org/10.1016/j.aei.2009.06.008

[21] Kammer, D. C. (2005). Sensor set expansion for modal vibration testing. *Mechanical Systems and Signal Processing*. https://doi.org/10.1016/j.ymssp.2004.06.003

[22] Lin, D. G., & Woo, S. M. (2007). Three dimensional analyses of deep excavation in Taipei 101 construction project. *Journal of GeoEngineering*, *2*(1), 29-42.

[23] Lee, F. H., Hong, S. H., Gu, Q., & Zhao, P. (2012). Application of large three-dimensional finite-element analyses to practical problems. *International Journal of Geomechanics*. https://doi.org/10.1061/(ASCE)GM.1943-5622.0000049

[24] Leung, E., Pappin, J., & Koo, R. (2010). Determination of small strain modulus and degradation for in-situ weathered rock and old alluvium deposits.

[25] Lim, A., Ou, C. Y., & Hsieh, P. G. (2010). Evaluation of clay constitutive models for analysis of deep excavation under undrained conditions. *Journal of GeoEngineering*, *5*(1), 9-20.

[26] Malings, C., & Pozzi, M. (2016). Value of information for spatially distributed systems: Application to sensor placement. *Reliability Engineering and System Safety*. https://doi.org/10.1016/j.ress.2016.05.010

[27] Moon, S. W., Hayashi, K., & Ku, T. (2017). Estimating spatial variations in bedrock depth and weathering degree in decomposed granite from surface waves. *Journal of Geotechnical and Geoenvironmental Engineering*. https://doi.org/10.1061/(ASCE)GT.1943-5606.0001679

[28] Moser, G., Paal, S. G., & Smith, I. F. C. (2017). Measurement system design for leak detection in hydraulic pressurized networks. *Structure and Infrastructure Engineering*. https://doi.org/10.1080/15732479.2016.1225312

Wang, Z. Z., Bertola, N. J., Goh, S. H., & Smith, I. F. C. (2021). Systematic selection of field response measurements for excavation back analysis. *Advanced Engineering Informatics*, *48*, 101296. https://doi.org/https://doi.org/10.1016/j.aei.2021.101296

[29] Ou, C. Y., Chiou, D. C., & Wu, T. S. (1996). Three-dimensional finite element analysis of deep excavations. *Journal of Geotechnical Engineering*. https://doi.org/10.1061/(asce)0733-9410(1996)122:5(337)

[30] Obrzud, R. F. (2010). On the use of the Hardening Soil Small Strain model in geotechnical practice. *Numerics in Geotechnics and Structures*, *16*.

[31] Phoon, K. K., & Kulhawy, F. H. (1999). Characterization of geotechnical variability. *Canadian Geotechnical Journal*. https://doi.org/10.1139/t99-038

[32] Papadimitriou, C., Beck, J. L., & Au, S. K. (2000). Entropy-based optimal sensor location for structural model updating. *JVC/Journal of Vibration and Control*. https://doi.org/10.1177/107754630000600508

[33] Papadimitriou, C. (2004). Optimal sensor placement methodology for parametric identification of structural systems. *Journal of Sound and Vibration*. https://doi.org/10.1016/j.jsv.2003.10.063

[34] Popper, K. (2005). The logic of scientific discovery. In *The Logic of Scientific Discovery*. https://doi.org/10.4324/9780203994627

[35] Papadopoulou, M., Raphael, B., Smith, I. F. C., & Sekhar, C. (2014). Hierarchical sensor placement using joint entropy and the effect of modeling error. *Entropy*. https://doi.org/10.3390/e16095078

[36] Pasquier, R., Goulet, J. A., & Smith, I. F. C. (2017). Measurement system design for civil infrastructure using expected utility. *Advanced Engineering Informatics*. https://doi.org/10.1016/j.aei.2016.12.002

[37] Proverbio, M., Costa, A., & Smith, I. F. C. (2018). Adaptive Sampling Methodology for Structural Identification Using Radial-Basis Functions. *Journal of Computing in Civil Engineering*. https://doi.org/10.1061/(ASCE)CP.1943-5487.0000750

[38] Rasmussen, C. E. (2004). Gaussian Processes in machine learning. *Lecture Notes in Computer Science (Including Subseries Lecture Notes in Artificial Intelligence and Lecture Notes in Bioinformatics)*. https://doi.org/10.1007/978-3-540-28650-9_4

[39] Rahardjo, H., Aung, K. K., Leong, E. C., & Rezaur, R. B. (2004). Characteristics of residual soils in Singapore as formed by weathering. *Engineering Geology*. https://doi.org/10.1016/j.enggeo.2004.01.002

Wang, Z. Z., Bertola, N. J., Goh, S. H., & Smith, I. F. C. (2021). Systematic selection of field response measurements for excavation back analysis. *Advanced Engineering Informatics*, *48*, 101296. https://doi.org/https://doi.org/10.1016/j.aei.2021.101296

[40] Robert-Nicoud, Y., Raphael, B., & Smith, I. F. C. (2005). Configuration of measurement systems using Shannon's entropy function. *Computers and Structures*. https://doi.org/10.1016/j.compstruc.2004.11.007

[41] Rechea, C., Levasseur, S., & Finno, R. (2008). Inverse analysis techniques for parameter identification in simulation of excavation support systems. *Computers and Geotechnics*. https://doi.org/10.1016/j.compgeo.2007.08.008

[42] Rahardjo, H., Satyanaga, A., Leong, E. C., Ng, Y. S., & Pang, H. T. C. (2012). Variability of residual soil properties. *Engineering Geology*. https://doi.org/10.1016/j.enggeo.2012.05.009

[43] Reale, C., Gavin, K., Librić, L., & Jurić-Kaćunić, D. (2018). Automatic classification of fine-grained soils using CPT measurements and Artificial Neural Networks. *Advanced Engineering Informatics*. https://doi.org/10.1016/j.aei.2018.04.003

[44] Sidak, Z. (1967). Rectangular Confidence Regions for the Means of Multivariate Normal Distributions. *Journal of the American Statistical Association*. https://doi.org/10.2307/2283989

[45] Sun, Y., Jiang, Q., Yin, T., & Zhou, C. (2018). A back-analysis method using an intelligent multi-objective optimization for predicting slope deformation induced by excavation. *Engineering Geology*. https://doi.org/10.1016/j.enggeo.2018.03.019

[46] Pai, S. G. S., Sanayei, M., & Smith, I. F. C. (2021). Model-Class Selection Using Clustering and Classification for Structural Identification and Prediction. *Journal of Computing in Civil Engineering*. https://doi.org/10.1061/(asce)cp.1943-5487.0000932

[47] Tien Bui, D., Nhu, V. H., & Hoang, N. D. (2018). Prediction of soil compression coefficient for urban housing project using novel integration machine learning approach of swarm intelligence and Multi-layer Perceptron Neural Network. *Advanced Engineering Informatics*. https://doi.org/10.1016/j.aei.2018.09.005

[48] Veijayaratnam, M., Poh, K. B., & Tan, S. L. (1993). Seismic Velocities in Singapore Soils and some Geotechnical Application. In *11th Southeast Asian Geotechnical Conference*.

[49] Vardon, P. J., Liu, K., & Hicks, M. A. (2016). Reduction of slope stability uncertainty based on hydraulic measurement via inverse analysis. *Georisk*. https://doi.org/10.1080/17499518.2016.1180400

Wang, Z. Z., Bertola, N. J., Goh, S. H., & Smith, I. F. C. (2021). Systematic selection of field response measurements for excavation back analysis. *Advanced Engineering Informatics*, *48*, 101296. https://doi.org/https://doi.org/10.1016/j.aei.2021.101296

[50] Wang, Z. Z., Goh, S. H., Koh, C. G., & Smith, I. F. (2018). Soil parameter identification for excavations: A falsification approach. *Numerical Methods in Geotechnical Engineering IX*. https://doi.org/10.1201/9781351003629-149

[51] Wang, Z.-Z., Goh, S. H., Koh, C. G., & Smith, I. F. C. (2019). An efficient inverse analysis procedure for braced excavations considering three-dimensional effects. *Computers and Geotechnics*, *107*. https://doi.org/10.1016/j.compgeo.2018.12.004

[52] Wang, Z. Z., Goh, S. H., Koh, C. G., & Smith, I. F. C. (2020). Comparative study of the effects of three data-interpretation methodologies on the performance of geotechnical back analysis. *International Journal for Numerical and Analytical Methods in Geomechanics*. https://doi.org/10.1002/nag.3120

[53] Xuan, F., Xia, X. H., & Wang, J. H. (2009). The application of a small strain model in excavations. *Journal of Shanghai Jiaotong University (Science)*, *14*(4), 418-422.

[54] Yuen, K. V., & Mu, H. Q. (2012). A novel probabilistic method for robust parametric identification and outlier detection. *Probabilistic Engineering Mechanics*. https://doi.org/10.1016/j.probengmech.2012.06.002

[55] Zdravkovic, L., Potts, D. M., & St. John, H. D. (2005). Modelling of a 3D excavation in finite element analysis. *Geotechnique*. https://doi.org/10.1680/geot.2005.55.7.497

[56] Zhang, W. G., & Goh, A. T. C. (2013). Multivariate adaptive regression splines for analysis of geotechnical engineering systems. *Computers and Geotechnics*. https://doi.org/10.1016/j.compgeo.2012.09.016

[57] Zhang, W., Goh, A. T., & Zhang, Y. (2015). Updating soil parameters using spreadsheet method for predicting wall deflections in braced excavations. *Geotechnical and Geological Engineering*, *33*(6), 1489-1498.

[58] Zhang, W., Zhang, Y., & Goh, A. T. (2017). Multivariate adaptive regression splines for inverse analysis of soil and wall properties in braced excavation. *Tunnelling and Underground Space Technology*, *64*, 24-33.

[59] Zhang, Y., Li, Y. E., & Ku, T. (2019). Geotechnical site investigation for tunneling and underground works by advanced passive surface wave survey. *Tunnelling and Underground Space Technology*. https://doi.org/10.1016/j.tust.2019.05.003